# A noncanonical function of cGAMP in inflammasome priming and activation

Karen V. Swanson,[1,2] Robert D. Junkins,[1,2] Cathryn J. Kurkjian,[1,2] Elizabeth Holley-Guthrie,[1,2] Avani A. Pendse,[3] Rachid El Morabiti,[6] Alex Petrucelli,[1,2] Glen N. Barber,[7] Chris A. Benedict,[6] and Jenny P.-Y. Ting[1,2,4,5]

[1]Lineberger Comprehensive Cancer Center, [2]Department of Genetics, [3]Division of Surgical Pathology, Department of Pathology and Laboratory Medicine, [4]Center for Translational Immunology, and [5]Institute for Inflammatory Diseases, University of North Carolina at Chapel Hill, Chapel Hill, NC
[6]Division of Immune Regulation, La Jolla Institute for Allergy and Immunology, La Jolla, CA
[7]Department of Cell Biology and Sylvester Comprehensive Cancer Center, University of Miami School of Medicine, Miami, FL

**Recognition of pathogen-associated molecular patterns and danger-associated molecular patterns by host cells is an important step in innate immune activation. The DNA sensor cyclic guanosine monophosphate–adenosine monophosphate (cGAMP) synthase (cGAS) binds to DNA and produces cGAMP, which in turn binds to stimulator of interferon genes (STING) to activate IFN-I. Here we show that cGAMP has a noncanonical function in inflammasome activation in human and mouse cells. Inflammasome activation requires two signals, both of which are activated by cGAMP. cGAMP alone enhances expression of inflammasome components through IFN-I, providing the priming signal. Additionally, when combined with a priming signal, cGAMP activates the inflammasome through an AIM2, NLRP3, ASC, and caspase-1 dependent process. These two cGAMP-mediated functions, priming and activation, have differential requirements for STING. Temporally, cGAMP induction of IFN-I precedes inflammasome activation, which then occurs when IFN-I is waning. In mice, cGAS/cGAMP amplify both inflammasome and IFN-I to control murine cytomegalovirus. Thus, cGAMP activates the inflammasome in addition to IFN-I, and activation of both is needed to control infection by a DNA virus.**

## INTRODUCTION

The inflammasome and type I interferon (IFN-I) pathways are two seminal routes by which innate immunity is activated to combat a wide variety of microbial pathogens. The inflammasome is a multimeric protein complex that includes an effector molecule that typically senses or recognizes either a pathogen-associated molecular pattern (PAMP) when encountering a microbial pathogen or danger-associated molecular pattern (DAMP) in the case of sterile inflammation, which arises in the absence of microbial infection (Martinon et al., 2002). With a few exceptions, inflammasome activation typically requires two activation steps (Guo et al., 2015; Broz and Dixit, 2016). The first step has been referred to as priming, in which activators such as TLRs or TNF induce transcription factors including NF-κB to activate the transcription of inflammasome-encoding genes such as *Nlrp3*, *Casp1*, and *pro-IL1b* and their subsequent translation (Bauernfeind et al., 2009). A second signal that is recognized by the effector molecule then causes inflammasome assembly. The assembled inflammasome is made up of an effector molecule, typically the adaptor molecule ASC, and pro-caspase-1. The activated effector molecules form a nucleating platform on which ASC polymerizes to form a fibril (Cai et al., 2014a; Lu et al., 2014; Sborgi et al., 2015). Caspase-1 then binds to ASC and oligomerizes. This assembled multimeric structure causes the proximal cleavage and activation of pro-caspase-1 to caspase-1, which then cleaves its target substrates, most prominent of which are pro-IL-1β and pro-IL-18. The effector molecule that provides specificity is typically an NLR protein. However, DNA ligands are recognized by a non-NLR protein, AIM2, and RIG-I–dependent inflammasome has also been reported (Bürckstümmer et al., 2009; Fernandes-Alnemri et al., 2009; Hornung et al., 2009; Roberts et al., 2009; Poeck et al., 2010). Although some inflammasome effector molecules have limited specificity such as AIM2, inflammasome activation in macrophages by a plethora of activators—such as nucleic acid, pore-forming toxins, changes in intracellular potassium or calcium, metabolic products, silica, and osmotic pressure—are dependent on the effector NLRP3 (Sutterwala et al., 2014). In addition to the canonical caspase-1 inflammasome, a noncanonical caspase-11 inflammasome is activated by intracellular LPS and requires NLRP3 for its activation (Kayagaki et al., 2011).

Correspondence to Jenny P.-Y. Ting: jenny_ting@med.unc.edu

A.A. Pendse's present address is Dept. of Pathology, Duke University Medical Center, Durham, NC.

Abbreviations used: BALF, bronchoalveolar lavage fluid; BMDM, bone marrow–derived macrophage; CDN, cyclic dinucleotide; cGAMP, cyclic GMP-AMP; cGAS, cyclic GAMP synthase; DAMP, danger-associated molecular pattern; DC, dendritic cell; DKO, double KO; MCMV, murine CMV; PAMP, pathogen-associated molecular pattern; qPCR, quantitative PCR; STING, stimulator of interferon genes.



The Rockefeller University Press
J. Exp. Med. 2017 Vol. 214 No. 12 3611–3626
https://doi.org/10.1084/jem.20171749



The Journal of Experimental Medicine

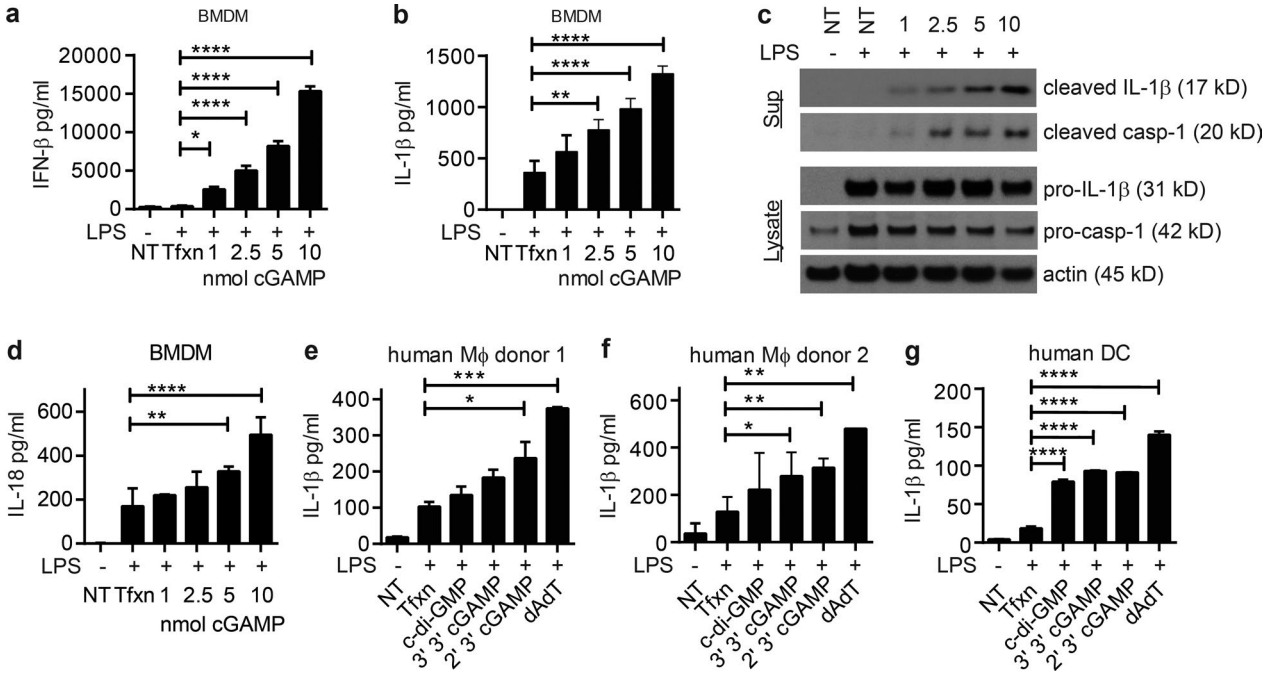


Figure 1. **cGAMP induces inflammasome activation.** (a and b) IFN-β (a) and IL-1β (b) ELISAs of BMDM supernatants primed with LPS then transfected with various dosages of cGAMP ($n$ = 3 independent experiments, mean ± SEM). (c) Western blots of supernatants and cell lysates from b. (d) IL-18 ELISA of BMDMs treated as described in a. (e–g) ELISAs of primary human macrophages (e and f) and human DCs (g) treated as depicted for BMDMs (individual donors ± SD). casp-1, caspase-1; Mφ, macrophage, NT, not transfected with PAMP; Tfxn, transfected with transfection reagent only. *, P < 0.05; **, P < 0.01; ***, P < 0.001; ****, P < 0.0001. Results shown in a, b, and d are combined from three independent experiments and are presented as the mean ± SEM.

The pathway that leads to DNA-induced IFN production is another route by which innate immunity is activated and has been well elucidated (Barber, 2014; Bhat and Fitzgerald, 2014; Cai et al., 2014b). The activation of IFN-I by DNA via the stimulator of interferon genes (STING) pathway involves several novel molecules that only recently have been unveiled (Ishikawa and Barber, 2008; Jin et al., 2008; Zhong et al., 2008). In this pathway, intracellular cytosolic DNA that arises from microbial pathogens is directly recognized by the enzyme cyclic GMP-AMP (cGAMP) synthase (cGAS), which leads to its dimerization and enzyme activation, with the ultimate production of the second messenger cyclic dinucleotide, 2′3′-cGAMP (Sun et al., 2013; Wu et al., 2013). Once produced, cGAMP binds to it downstream effector, STING, leading to its association and activation of TBK1, which triggers the subsequent phosphorylation and activation of IRF3. This results in IRF3-dimerization, nuclear translocation, and engagement of IFN-I promoter, leading to IFN-I transcription. The details of this pathway have been supported by multiple studies and are now widely accepted (Barber, 2014; Bhat and Fitzgerald, 2014; Cai et al., 2014b). In addition to IFN-I production, cGAMP binding to STING induces expression of NF-kB, leading to TNF and IL-6 expression (Ahn et al., 2012). Recently, inflammasome activation has been shown to negatively regulate cGAS activity by caspase cleavage of cGAS (Wang et al., 2017); however, positive cross-talk between inflammasome and cGAS in innate immunity has not been documented. In this work, we show for the first time that the second messenger cGAMP not only activates IFN-I, but also activates inflammasomes via an AIM2-NLRP3-ASC–dependent pathway. Furthermore, we show that dAdT dsDNA relies on this pathway to amplify the inflammasome for cytokine secretion without altering pyroptosis. During murine CMV (MCMV) infection, host cells are dependent on both arms of cGAMP signaling pathways, IFN-I and inflammasome, for control of the infection. This suggests that cGAMP contributes to two key innate immune pathways that are known to play keys roles in numerous pathogen infections.

## RESULTS

### 2′3′-cGAMP induces secretion of IL-1β and IL-18

To investigate whether 2′3′-cGAMP induces inflammasome formation, mouse bone marrow–derived macrophages (BMDMs) were primed with LPS to induce signal 1, followed by transfection with increasing concentrations of 2′3′-cGAMP. As expected, BMDMs secreted large amounts of IFN-β 6 h poststimulation (Fig. 1 a). Unexpectedly, BMDMs induced the activation of caspase-1 and secreted significant amounts of the inflammasome-dependent cytokines IL-1β and IL-18 in response to 2′3′-cGAMP in a dose-dependent fashion (Fig. 1, b–d). To determine whether human macro-

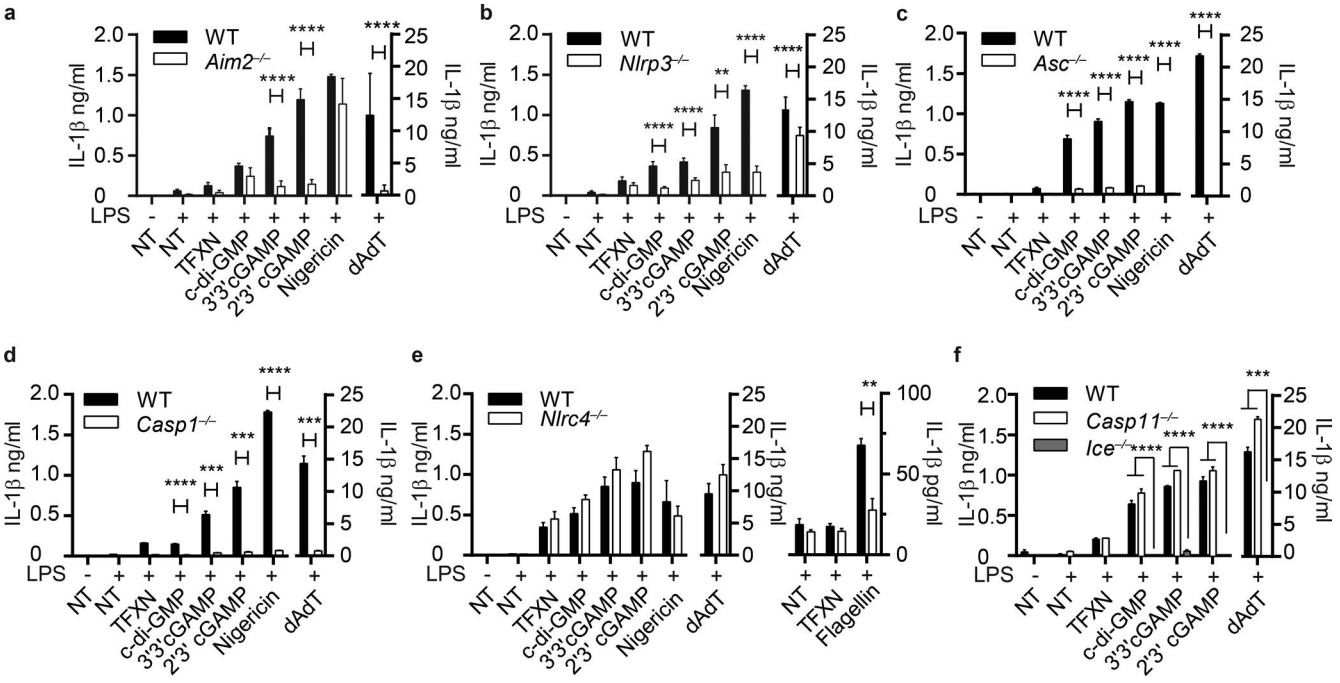


Figure 2. **cGAMP induces AIM2–NLRP3–ASC inflammasome.** IL-1β ELISAs from supernatants of LPS-primed BMDMs transfected with the indicated PAMP or DAMP. BMDMs were obtained from WT or *Aim2*$^{-/-}$ (a), *Nlrp3*$^{-/-}$ (b), *Asc*$^{-/-}$ (c), *Casp1*$^{-/-}$ (d), *Nlrc4*$^{-/-}$ (e), and *Casp11*$^{-/-}$ and *Ice*$^{-/-}$ (f). NT, not transfected with PAMP; TFXN, transfected with transfection reagent only. $n = 3$ independent experiments ± SEM. **, $P < 0.01$; ***, $P < 0.001$; ****, $P < 0.0001$.

phages and dendritic cells (DCs) respond to 2′3′-cGAMP in a fashion similar to mouse BMDMs, we purified primary macrophages from two donors and primary DCs from a third donor. Both sets of primary human macrophages and the primary human DCs secreted significant amounts of IL-1β in response to 2′3′-cGAMP (Fig. 1, e–g). Primary human DCs also secreted significant levels of IL-1β in response to the bacterial-derived cyclic dinucleotides (CDNs), c-di-GMP and 3′3′-cGAMP, but less than the canonical 2′3′-cGAMP. These data show that 2′3′-cGAMP, in addition to its known role as an inducer of IFN-β, induces the activation of caspase-1 and secretion of IL-1β and IL-18, two inflammasome-dependent cytokines. These data strongly suggest that the second messenger 2′3′-cGAMP, in addition to other bacterial CDNs (Abdul-Sater et al., 2013), can induce inflammasome formation.

### 2′3′-cGAMP inflammasome composition and formation

We next investigated the inflammasome pathways that were activated by 2′3′-cGAMP. BMDMs were generated from mice deficient in various inflammasome components, stimulated with LPS, and then transfected with 2′3′-cGAMP or other inflammasome-inducing stimuli as controls. The positive controls, AIM2-inducing ligand dAdT and NLRP3-inducing stimulant nigericin, acted as expected. Inflammasome activation by dAdT was dependent on Aim2, Asc, and caspase-1 but not Nlrc4 and caspase-11, as determined by IL-1β secretion (Fig. 2, a–f), whereas activation by nigericin was dependent on Nlrp3, Asc, and caspase-1 but not Aim2, Nlrc4, and caspase-11. This result is consistent with prior findings that Aim2 is specifically required for DNA-activated inflammasome, whereas Nlrp3 is required for nigericin-activated inflammasome. In contrast, the loss of either Aim2 or Nlrp3 had a significant effect on 2′3′-cGAMP–induced IL-1β secretion (Fig. 2, a and b). cGAMP stimulation of BMDMs from *Aim2*$^{-/-}$ or *Nlrp3*$^{-/-}$ mice had a significant reduction of IL-1β secretion compared with WT mice. Additionally, inflammasome activation by 2′3′-cGAMP was completely dependent on ASC and caspase-1, as BMDM from *Asc*$^{-/-}$ and *Casp1*$^{-/-}$ mice did not secrete IL-1β in response to 2′3′-cGAMP (Fig. 2, c, d, and f). The loss of Nlrc4, which senses flagellin and type 3 secretory proteins through NAIP proteins, had no effect on IL-1β secretion after cGAMP transfection (Fig. 2 e).

Recently, several studies showed that caspase-11 is involved in a noncanonical NLRP3-dependent inflammasome that is activated by intracellular LPS (Kayagaki et al., 2011; Aachoui et al., 2013; Rühl and Broz, 2015). Because we found that Nlrp3 was important for the 2′3′-cGAMP–induced inflammasome, we investigated the need for caspase-11. As shown in Fig. 2 f, inflammasome activation by 2′3′-cGAMP is intact in *Casp11*$^{-/-}$ mice, but it is lost in *Ice*$^{-/-}$ mice, which lacked both caspase-1 and caspase-11, suggesting that 2′3′-cGAMP and the bacterial derived CDNs induce a canonical inflammasome.

The NLRP3 inflammasome can be induced by multiple stressors to the cell. Many of these different pathways are thought to converge on $K^+$ mobilization to induce the

activation of the NLRP3 inflammasome (Muñoz-Planillo et al., 2013). We investigated which NLRP3 pathway was important for 2′3′-cGAMP–induced inflammasome activation. BMDMs were primed with LPS and then treated with inflammasome inhibitors for 30 min before cGAMP transfection. 2′3′-cGAMP–induced inflammasome activation was sensitive to 2-APB, an inhibitor of ER $Ca^{2+}$ release, and *N*-acetyl-L-cysteine, a scavenger of ROS (Fig. S1, a and b). The addition of extracellular KCl prevents $K^+$ mobilization. Because high amounts of extracellular KCl killed BMDMs by 6 h, the assay was modified to add extracellular KCl for the last 1, 2, or 3 h of a 5-h inflammasome activation experiment. Extracellular KCl addition for the final 2 and 3 h significantly inhibited 2′3′-cGAMP–induced IL-1β secretion (Fig. S1 c). These data show that cGAMP-induced inflammasome responds to multiple NLRP3 inflammasome inhibitors and is dependent on ROS and mobilization of $Ca^{2+}$ and $K^+$.

### 2′3′-cGAMP induces inflammasome components to colocalize in cells without inducing cell death

The functional data show that 2′3′-cGAMP induces both AIM2- and NLRP3-dependent inflammasomes in that the loss of AIM2 or NLRP3 causes a significant reduction in cGAMP-induced IL-1β secretion. This suggests that AIM2- and NLRP3-dependent inflammasome complexes are formed within the same cell. To investigate this possibility, BMDMs were LPS-primed, followed by transfection with cGAMP. Fig. 3 a shows that IL-1β secretion after transfection of *Aim2*$^{-/-}$ *Nlrp3*$^{-/-}$ double KO (DKO) BMDMs with 2′3′-cGAMP is significantly less (95% reduction) than that of WT BMDMs (Fig. 3 a). Inflammasome activation can lead to cell death via pyroptosis, so we need to examine this aspect to perform microscopic examination (He and Amer, 2014). Release of adenylate cyclase was measured to determine the amount of cell death induced during inflammasome activation. As shown in Fig. 3 b, dAdT and nigericin induced significant amounts of cell death, whereas cell death induced by cGAMP was barely detectable and insignificant. There were no differences between BMDMs from WT and *Aim2*$^{-/-}$ or *Nlrp3*$^{-/-}$ mice after cGAMP transfection (Fig. 3 c). This result shows that cGAMP differs from most inflammasome-inducing stimuli in that it does not induce pyroptosis.

We next used confocal microscopy to investigate whether 2′3′-cGAMP induces Aim2 and Nlrp3 to colocalize with Asc specks. A mouse DC cell line, JAWSII, was transduced with AIM2-Flag under a doxycycline promoter. Cells were pulsed with doxycycline to induce low levels of AIM2-Flag during the LPS-priming step. Doxycycline was washed out before the cells were transfected with a 30:1 mixture of unlabeled 2′3′-cGAMP and fluorescein-labeled 2′3′-cGAMP (cGAMP-FL). Asc, Aim2, Nlrp3, and 2′3′-cGAMP-FL were all found to colocalize, suggesting that 2′3′-cGAMP induces inflammasome complexes composed of both AIM2 and NLRP3 in addition to the common adaptor, Asc (Fig. 3, d and e; and Fig. S2, a and b).

### cGAS/cGAMP amplifies AIM2 inflammasomes

Because 2′3′-cGAMP is produced after cytosolic DNA is detected by cGAS, we investigated the role of cGAS in the DNA-sensed AIM2 inflammasome. Fig. 4 a illustrates how cytosolic DNA can be sensed via AIM2, which is well documented, and via the cGAMP pathway described here, and their proposed inflammasome-dependent outcomes. DNA is known to bind AIM2, leading to inflammasome activation (Jin et al., 2012). In addition, DNA binds and activates cGAS to cause cGAMP activation, which is shown in this study to induce inflammasome activation. When either sensor is lost, corresponding losses in inflammasome-dependent cytokines are anticipated. We used JAWSII cells that are derived from mouse DCs, with and without sh-cGAS, to investigate the role of cGAS in DNA-induced inflammasomes. We were able to achieve 75% knockdown of *cGAS* in the JAW SII sh-cGAS cells (Fig. 4 b). These cells were LPS-primed followed by transfection with dAdT. As expected, dAdT induced IFN-β in the JAWSII cells and was significantly reduced in the presence of sh-cGAS (Fig. 4 c). Importantly, IL-1β secretion after dAdT transfection was partially dependent on cGAS, as IL-1β levels from JAWSII sh-cGAS were significantly reduced compared with WT (Fig. 4 d). This is consistent with the model in Fig. 4 a, depicting a scenario in which DNA activates cGAS, which then leads to cGAMP production, which causes inflammasome activation. We also used BMDMs from both WT and *cGAS*$^{-/-}$ mice to determine the role of cGAS in inflammasome activation. BMDMs were LPS-primed and transfected with CDNs and dAdT, or nigericin as a negative control. Because nigericin does not act through cGAS, the loss of cGAS had no effect on either IL-1β or IFN-β production (Fig. 4, e and f). We expected that when stimulated with CDNs, there would be no difference in IL-1β or IFN-β secreted from WT or *cGAS*$^{-/-}$ BMDMs, because CDNs are downstream of cGAS in the DNA-sensing pathway. As anticipated, there was no difference in the levels of IL-1β or IFN-β when *cGAS*$^{-/-}$ cells were stimulated with CDNs, including the canonical 2′3′-cGAMP (Fig. 4, e and f). IFN-β production from dAdT, however, was dependent on cGAS, as loss of cGAS significantly reduced IFN-β (Fig. 4 f). This suggests that most of the IFN-β production via dAdT sensing is through the cGAS pathway. Importantly, IL-1β secretion after dAdT transfection was partially dependent on cGAS, likely via cGAMP, as IL-1β levels from *cGAS*$^{-/-}$ BMDMs were significantly reduced compared with WT (Fig. 4 e). The absence of a larger difference can be explained by the direct activation of AIM2 by DNA in these cells, which represent the first pathway of DNA-activated inflammasome depicted in the model shown in Fig. 4 a.

Because our data suggest that cGAMP is involved in DNA-induced inflammasome activation, we needed to de-

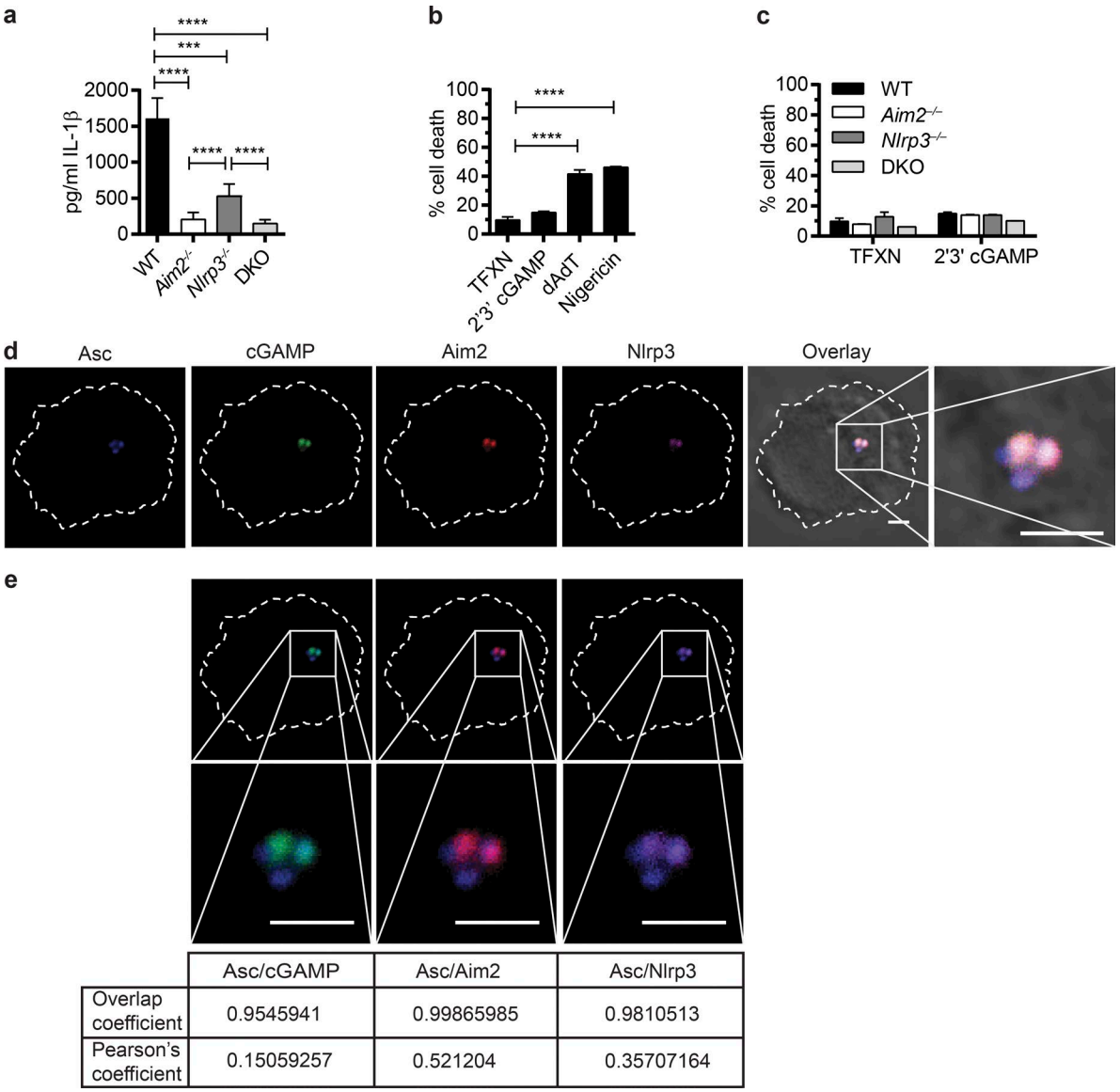


| | Asc/cGAMP | Asc/Aim2 | Asc/Nlrp3 |
|---|---|---|---|
| Overlap coefficient | 0.9545941 | 0.99865985 | 0.9810513 |
| Pearson's coefficient | 0.15059257 | 0.521204 | 0.35707164 |

Figure 3. **cGAMP induces complexes containing both NLRP3 and AIM2.** WT, *Aim2*$^{-/-}$, *Nlrp3*$^{-/-}$, or *Aim2*$^{-/-}$ *Nlrp3*$^{-/-}$ DKO BMDMs were LPS-primed followed by transfection with cGAMP or indicated PAMPs or DAMPs. (a–c) IL-1β ELISA (a) and cell death (b and c) as measured by adenylate cyclase release in supernatants. $n = 3$ independent experiments, mean ± SEM. ***, $P < 0.001$; ****, $P < 0.0001$. TFXN, transfected with transfection reagent without DAMP. (d and e) Confocal microscopy of JAWSII cells expressing AIM2-Flag pulsed with doxycycline during LPS priming followed by transfection with a 30:1 mixture of 2′3′-cGAMP and fluorescein-labeled 2′3′-cGAMP. Cells were labeled with primary antibodies to Asc, Nlrp3, and Flag (for Aim2-Flag) followed by Alexa Fluor–labeled secondary antibodies. Shown are pseudocolored images: blue, ASC; green, fluorescein-labeled 2′3′-cGAMP; red, AIM2-Flag; magenta, NLRP3. (e) Colocalization analysis and images of Asc versus cGAMP, Aim2, or Nlrp3 as indicated, from the slice shown in d. Overlap coefficient and Pearson's correlation coefficient were determined using ImageJ. Bars, 2 μm.

termine whether cGAMP directly interacts with components of the DNA-induced AIM2 inflammasome during dAdT stimulation. Therefore, we investigated whether 2′3′-cGAMP associates with dAdT-induced AIM2 inflammasomes by confocal microscopy. JAWSII AIM2-Flag cells were doxycycline-induced during the LPS priming as in Fig. 3 c. The cells were then cotransfected with cGAMP-FL at a low dose that does not induce IL-1β, along with dAdT. Confocal microscopy shows that cGAMP-FL colocalized to the same inflammasome complex as dAdT, AIM2, and caspase-1 (Fig. 4 g and Fig. S2 c). These data show that full activation of the inflammasome by dAdT is dependent on cGAS DNA sensing and 2′3′-cGAMP production. 2′3′-cGAMP colocalizes with the same AIM2 inflammasome as dAdT and functionally acts to enhance and amplify DNA-sensed inflammasome activity.

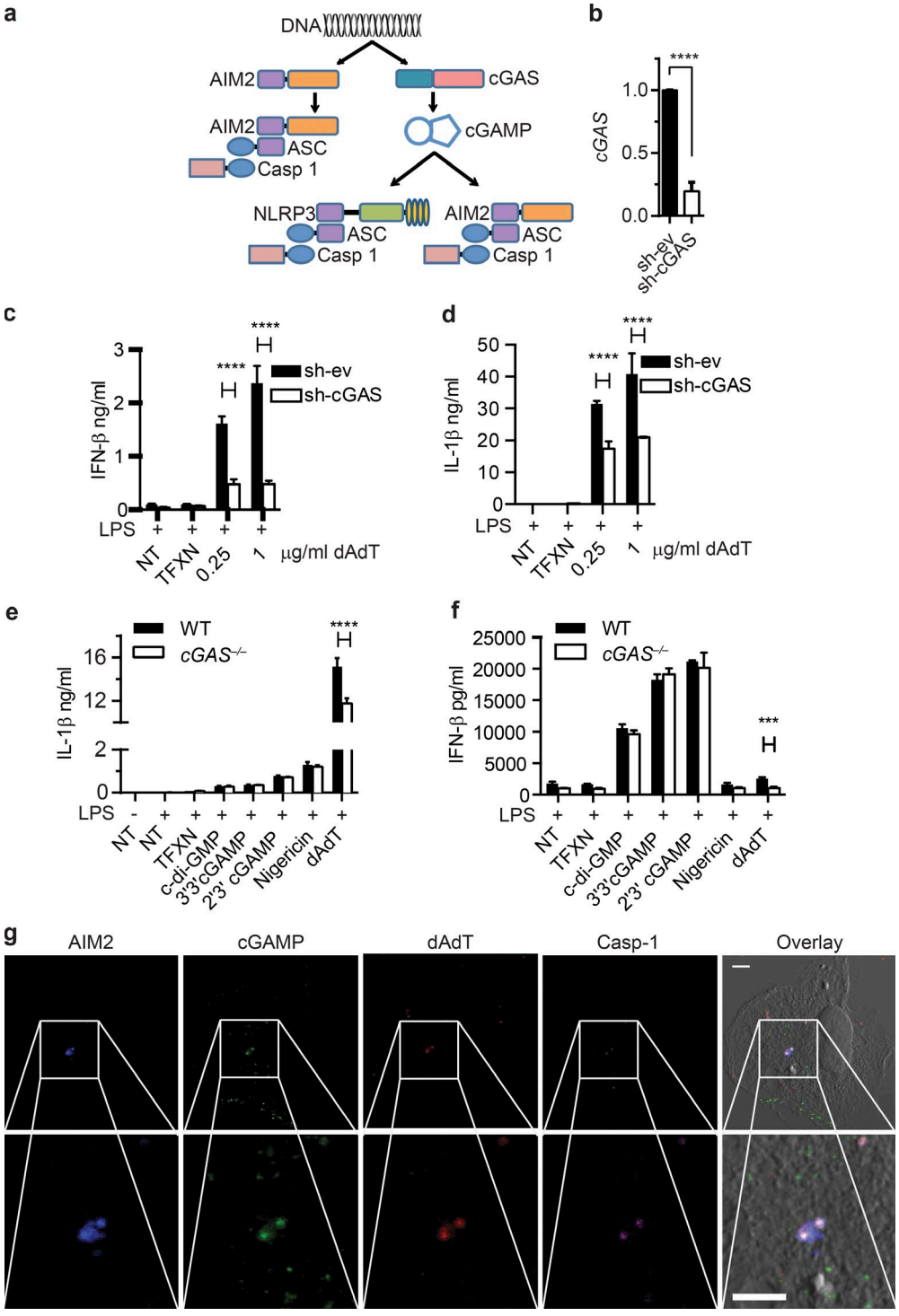


Figure 4. **cGAS is important for DNA–induced inflammasome.** (a) Pathways that can be activated by dsDNA to activate the inflammasome. To the left is the published AIM2-dependent pathway. To the right is the proposed pathway mediated by cGAMP. (b) Relative *cGAS* as determined by qPCR of JAWSII cells containing empty vector (sh-ev) or shRNA targeting cGAS (sh-cGAS). (c) IFN-β or (d) IL-1β levels of supernatants from JAWSII DCs primed with LPS then transfected with dAdT, transfection reagent alone (TFXN), or not treated (NT). (e and f) IL-1β (e) or IFN-β (f) levels of supernatants from BMDM primed with LPS then transfected with the indicated PAMP or DAMP, or not transfected (NT). $n = 3$ independent experiments, mean ± SEM. ***, $P < 0.001$; ****, $P < 0.0001$. (g) Confocal microscopy of LPS-primed JAWSII cells expressing AIM2-Flag transfected with 10 μg/ml dAdT and 130 pmol fluorescein-labeled 2′3′-cGAMP for 4 h. During the final hour, FLICA-660 was added to detect caspase-1. Bars, 5 μm. Cells were imaged on a Zeiss 700 confocal microscope. Pseudocolors: blue, AIM2-Flag; green, fluorescein-labeled 2′3′-cGAMP; red, dAdT-rhodamine; and magenta, caspase-1.

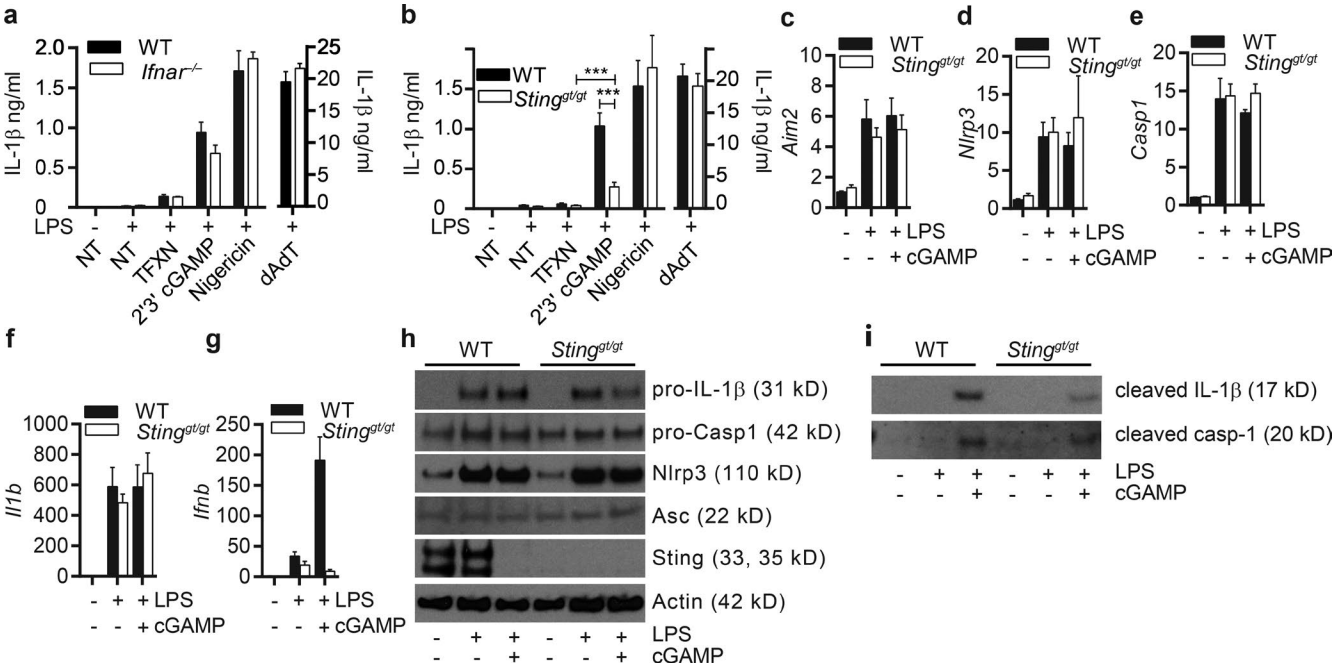


Figure 5. **cGAMP-induced inflammasome activation after LPS priming is partially dependent on Sting.** (a and b)WT and *Ifnar*$^{-/-}$ (a) or *Sting*$^{gt/gt}$ (b) BMDMs were LPS-primed followed by transfection with cGAMP as indicated for 6 h, and supernatants were measured for IL-1β. (c–g) mRNA levels as determined by qPCR of *Aim2* (c), *Nlrp3* (d), *Casp1* (e), *Il1b* (f), and *Ifnb* (g). (h and i) Immunoblots of lysates (h) or supernatants (i) from the same experiment. $n = 5$ independent experiments ± SEM. ***, $P < 0.001$. casp-1, caspase-1; NT, not treated; TFXN, transfected with transfection reagent only.

**Sting is required for optimal cGAMP-induced inflammasome**

Several studies implicate the necessity of IFN-I for inflammasome activation by bacteria (reviewed in Malireddi and Kanneganti, 2013), although IFN-I, conversely, has been shown to inhibit NLRP3-dependent IL-1β production (Guarda et al., 2011). Because cGAMP binds to the adapter molecule STING to cause IFN-β production, we investigated whether Sting was also used by 2′3′-cGAMP for inflammasome activation by LPS and cGAMP, either directly by binding to Sting or indirectly by the necessity for IFN-β production. We first investigated whether IFN-I signaling is important for 2′3′-cGAMP inflammasome activation with the use of *Ifnar*$^{-/-}$ mice (Fig. 5 a). Because *Aim2* can be regulated by interferon, we tested whether the loss of *Ifnar* might reduce Aim2 up-regulation during the priming phase and thus have an effect on AIM2 inflammasome formation. As shown in Fig. 5 a, there was no defect in the inflammasome activation of IL-1β secretion when cells were stimulated with the AIM2 ligand dAdT in *Ifnar*$^{-/-}$ BMDMs compared with WT cells. However, the secretion of IL-1β was partially dependent on Sting, as cGAMP stimulation of BMDMs from Sting-deficient (*Sting*$^{gt/gt}$) mice had a significant reduction of IL-1β secretion compared with WT mice (Fig. 5 b). We next investigated whether LPS priming is modulated in Sting-deficient BMDMs. BMDMs were LPS-primed followed by cGAMP transfection. Inflammasome component mRNA levels were determined by quantitative PCR (qPCR), and protein levels by immunoblotting. As shown in Fig. 5 (c–f), mRNA levels for *Aim2*, *Nlrp3*, *Casp1*, and *IL-1β* were up-regulated after LPS stimulation and were equivalent between BMDMs from WT and *Sting*$^{gt/gt}$ mice. Inflammasome component mRNA levels remained unchanged after transfection of cGAMP into LPS-primed BMDMs in both WT and *Sting*$^{gt/gt}$ BMDMs. Control *Ifnb* levels after cGAMP transfection were significantly up-regulated in WT BMDMs but were unchanged in *Sting*$^{gt/gt}$ BMDMs, confirming a loss of Sting activity (Fig. 5 g). Protein levels of inflammasome components mirrored that of mRNA levels and were not changed by *Sting* deficiency (Fig. 5 h). Levels of pro-IL-1b, pro-caspase-1, and Nlrp3 were up-regulated and equivalent after LPS stimulation of both WT and *Sting*$^{gt/gt}$ BMDMs; importantly, the addition of cGAMP did not alter LPS priming levels. Sting protein was undetectable after cGAMP transfection, confirming published research that Sting is degraded after activation (Tao et al., 2016). There is a modest reduction in cleaved caspase-1 and more pronounced reduction in cleaved IL-1β in the supernatants of *Sting*$^{gt/gt}$ BMDMs versus WT after cGAMP transfection (Fig. 5 i), confirming the ELISA data. Together, these data suggest that during LPS priming, Sting does not act at the priming step of cGAMP-inflammasome activation, but it does affect IL-1β secretion. Future work is needed to fully elucidate its role.

### 2′3′-cGAMP primes expression of inflammasome components

Inflammasome formation and activation under most circumstances are thought of as a two-step process. The first signal primes the cell by up-regulating inflammasome components, and the second signal induces inflammasome formation and activation. Because our data show that cGAMP can act as the second signal to induce inflammasome activation, we next investigated whether it also has the ability to act as the first signal or priming step in inflammasome formation. We assessed the ability of 2′3′-cGAMP to prime the expression of mRNA encoding individual components of the inflammasome by qPCR. *Aim2*, *Nlrp3*, and *Casp1* transcripts were all significantly increased in response to 2′3′-cGAMP, and equally as well as with dAdT and the standard priming PAMP, LPS (Fig. 6, a–c). *Il1b* also was up-regulated in response to 2′3′-cGAMP and dAdT, but at significantly lower levels than LPS (Fig. 6 d). Transcript levels for the adapter molecule, *Asc,* remained unchanged during stimulation with 2′3′-cGAMP, dAdT, and LPS. This suggests that BMDMs have sufficient basal levels of ASC for inflammasome formation (Fig. 6 e). All three PAMPs increased levels of the positive control, *Ifnb*, as expected, with 2′3′-cGAMP increasing *Ifnb* significantly more than dAdT and LPS (Fig. 6 f). These results demonstrate that cGAMP can increase mRNA encoding key inflammasome components.

It has been previously shown by others that dAdT induction of the AIM2 inflammasome has the ability to self-prime and thus does not need a separate "signal one" for activation (Zhao et al., 2014). Because 2′3′-cGAMP induction of IL-1β secretion is AIM2 dependent and cGAMP increased the expression of inflammasome components to a similar degree as dAdT, we investigated whether cGAMP could act as both signal 1 and 2 and induce inflammasome activation without LPS priming. BMDMs were transfected with 2′3′-cGAMP, and IFN-β and IL-1β were detected by ELISA. At 6 h posttransfection, 2′3′-cGAMP induced the secretion of large amounts of IFN-β in a dose-dependent fashion (Fig. 6 g). By 19 h posttransfection, levels of IFN-β decreased dramatically to near untreated levels (Fig. 6 h). Although levels of IL-1β were detectable 6 h posttransfection, they were not significantly different from those of unstimulated cells (Fig. 6 i). However, by 19 h posttransfection, cGAMP dose-dependently induced significant amounts of IL-1β (Fig. 6 j). These data show that 2′3′-cGAMP can prime and up-regulate inflammasome components and activate inflammasomes without the need for an independent priming step.

Because cGAMP binding to STING induces the cytokines IFN-β and TNF, both of which are known to prime inflammasome components, we used Sting-deficient BMDMs to investigate the inflammasome priming induced by cGAMP. We also used *Ifnar*$^{-/-}$ BMDMs to determine the role of IFN-I during cGAMP priming. After cGAMP stimulation, IL-1β is significantly decreased to near-background levels in both *Sting*$^{gt/gt}$ and *Ifnar*$^{-/-}$ BMDMs, whereas IFN-β is undetectable in *Sting*$^{gt/gt}$ and significantly decreased in *Ifnar*$^{-/-}$ cells (Fig. 6, k and l). Although large amounts of Tnf were detected from WT BMDMs after cGAMP transfection, Tnf was undetectable from *Sting*$^{gt/gt}$ BMDMs and just above the level of detection from *Ifnar*$^{-/-}$ cells (Fig. 6 m). This result suggests that after cGAMP transfection, Tnf secretion is largely caused by IFN-I signaling. We then looked at the priming of inflammasome components by qPCR. Stimulation of both *Sting*$^{gt/gt}$ and *Ifnar*$^{-/-}$ BMDMs with cGAMP induced no transcript up-regulation of the inflammasome components *Aim2*, *Nlrp3*, *Casp1*, *Il1b*, and *Asc* (Fig. 6, n–r). Collectively, these data suggest that cGAMP's self-priming action is a result of its IFN-β production. This is distinct from LPS priming shown in Fig. 5, where Sting and Ifnar deficiency did not affect LPS-induced expression of inflammasome genes.

### 2′3′-cGAMP induces inflammasome activation in vivo

Because 2′3′-cGAMP can induce both signal 1 and 2 during inflammasome formation in vitro, it is important to investigate whether the same is true in vivo. 6–8-wk-old female mice were given two intranasal doses of 2′3′-cGAMP to mimic the in vitro protocol, where the cyclic dinucleotide served to both prime and activate the inflammasome. We favor this protocol over a conventional one where LPS is used to prime signal 1, because LPS alone can induce both signals 1 and 2 in mice, thus confounding the interpretation (Laudisi et al., 2013). Fig. 7 a shows that significant amounts of IL-1β were detected in mice treated with two doses of 2′3′-cGAMP compared with saline or cGAMP followed by saline, suggesting that indeed 2′3′-cGAMP induces inflammasome formation in vivo. In vivo inflammasome formation was dependent on both Nlrp3 and Aim2, as *Nlrp3*$^{-/-}$, *Aim2*$^{-/-}$, and *Nlrp3*$^{-/-}$ *Aim2*$^{-/-}$ mice secreted significantly less IL-1β in the bronchoalveolar lavage fluid (BALF; Fig. 7 b). Because our protocol collected BALF and serum 28 h after the first dose of cGAMP, we investigated whether these differences in IL-1β could be caused by differential recruitment of inflammasome-producing cells to the lungs. We found no difference in the amount of total macrophages in the BALF between the three KO strains and WT (Fig. S3). A significant amount of IFN-β was detected in BALF and serum from WT mice after intranasal 2′3′-cGAMP administration. However there was no difference in the amount of IFN-β detected in either BALF or serum between WT and *Nlrp3*$^{-/-}$, *Aim2*$^{-/-}$, or *Nlrp3*$^{-/-}$ *Aim2*$^{-/-}$ DKO mice, indicating that none of these genes are required for 2′3′-cGAMP–induced IFN-β production (Fig. 7, c and d). These data suggest that 2′3′-cGAMP induces AIM2- and NLRP3-dependent inflammasome formation in vivo.

### cGAS-dependent inflammasome activation is necessary for the control of MCMV

The data thus far show that cGAMP induces both IFN-β and inflammasome activation. We next addressed the necessity of both arms of cGAMP signaling in the control of a DNA virus.

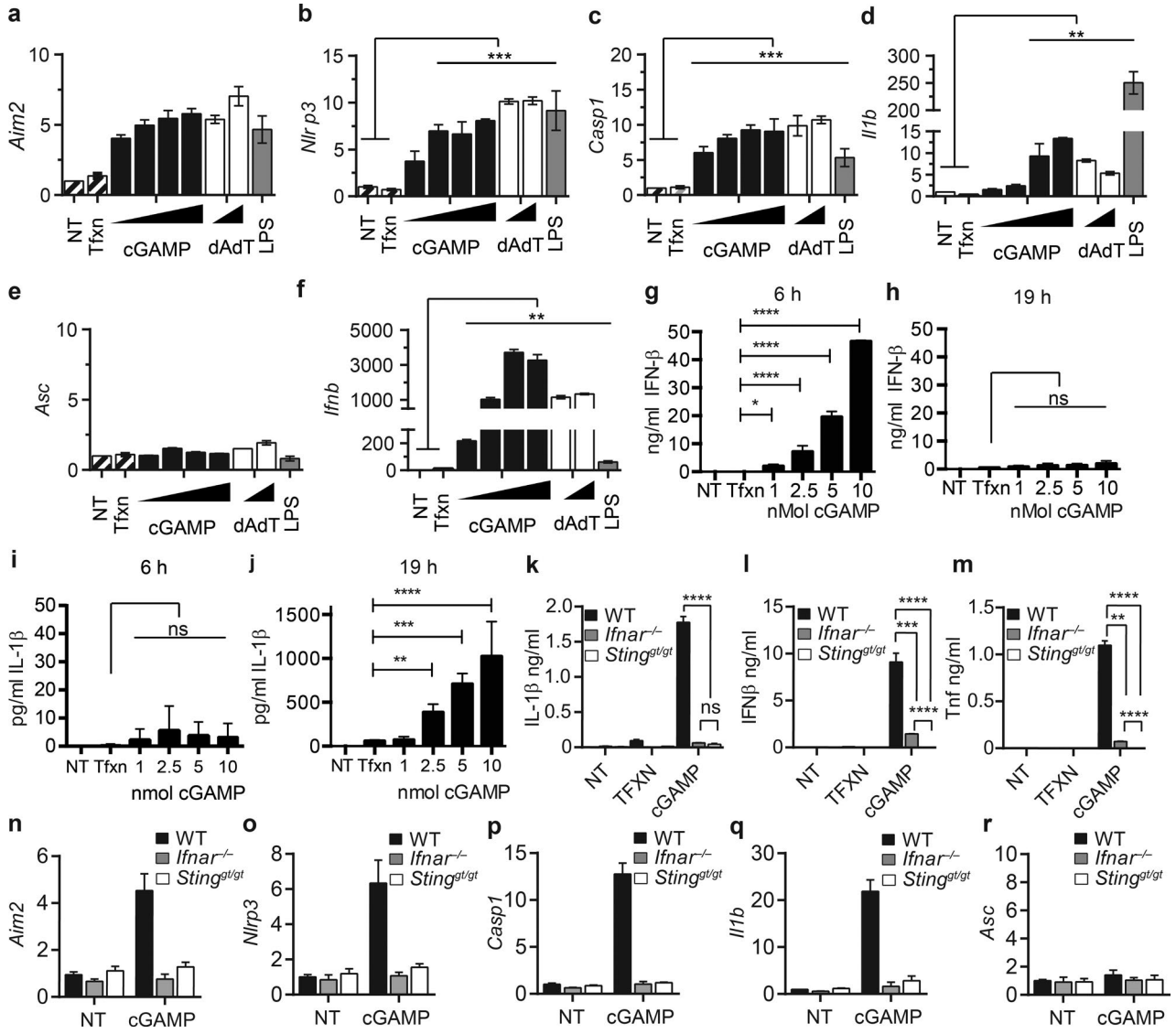


Figure 6. **cGAMP alone can serve as the priming signal by increasing mRNA levels for inflammasome components in a Sting- and Ifnar-dependent fashion.** BMDMs were transfected with increasing amounts of 2′3′-cGAMP, dAdT, or addition of 200 ng/ml LPS and analyzed after 6 h. (a–f) qPCR transcript levels of inflammasome components *Aim2*, *Nlrp3*, *Casp1*, *Il1b*, and *Asc* in addition to *Ifnb* produced by BMDM after treatment. $n = 3$ independent experiments. Shown is a representative with technical replicates of three, mean ± SD. (g–j) IFN-β (g and h) and IL-1β (i and j) in supernatants from BMDMs treated with increasing amounts of 2′3′-cGAMP for 6 h (g and i) and 19 h (h and j). NT, not treated. WT, *Ifnar*$^{-/-}$, or *Sting*$^{gt/gt}$ BMDMs were transfected with cGAMP, transfection reagent alone (TFXN), or not treated (NT) for 19 h. (k–m) IL-1β (k), IFN-β (l), or Tnf (m) levels of supernatants after treatment. (n–r) Transcript levels as measured by qPCR for inflammasome components *Aim2*, *Nlrp3*, *Casp1*, *Il1b*, and *Asc* produced by BMDMs after treatment. $n = 3$ independent experiments, mean ± SEM; ns, not significant; *, $P < 0.05$; **, $P < 0.01$; ***, $P < 0.001$; ****, $P < 0.0001$.

We selected MCMV because it has been shown to induce an Aim2 inflammasome (Rathinam et al., 2010). We investigated whether cGAS/cGAMP could enhance the inflammasome as predicted during MCMV infection in BMDMs. BMDMs were infected with MCMV, and inflammasome activation was determined by monitoring IL-1β secretion. Our data confirm that MCMV infection of WT BMDMs induces an Aim2 inflammasome (Fig. 8 a). Additionally, IL-1β secretion from MCMV-infected *cGAS*$^{-/-}$ BMDMs was significantly reduced compared with WT (Fig. 8 a). This confirms our data that cGAMP enhances the Aim2 inflammasome. To separate out antiviral effects that might be caused by cGAMP-induced IFN-I, we compared WT, *Ifnar*$^{-/-}$, and *Ifnar*$^{-/-}$ *cGAS*$^{-/-}$ DKO BMDMs. Fig. 8 b shows that there is no difference in IL-1β secretion between WT and *Ifnar*$^{-/-}$ BMDMs infected with MCMV. IL-1β peaked for both WT and *Ifnar*$^{-/-}$ BMDMs 2 d after MCMV infection and remained high for 3 d. However, the addition of cGAS deficiency in *Ifnar*$^{-/-}$ *cGAS*$^{-/-}$ DKO

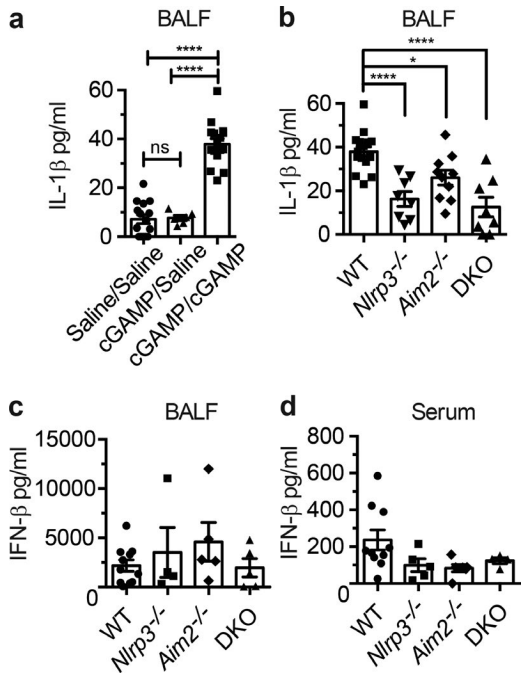


Figure 7. **cGAMP alone is sufficient to induce the inflammasome in vivo.** (a) IL-1β from BALF obtained from WT mice treated intranasally with cGAMP followed by saline or with cGAMP followed by cGAMP. (b) IL-1β from BALF obtained from WT, *Aim2*$^{-/-}$, *Nlrp3*$^{-/-}$, or *Aim2*$^{-/-}$ *Nlrp3*$^{-/-}$ DKO mice intranasally treated with cGAMP. (c and d) IFN-β ELISA from BALF or serum from WT and gene-deficient mice as in b. For cGAMP/cGAMP-treated: WT, $n = 17$; *Aim2*$^{-/-}$, $n = 10$; *Nlrp3*$^{-/-}$, $n = 8$; *Aim2*$^{-/-}$ *Nlrp3*$^{-/-}$ DKO, $n = 8$; for saline treated: WT, $n = 15$; *Aim2*$^{-/-}$, $n = 9$; *Nlrp3*$^{-/-}$, $n = 8$; *Aim2*$^{-/-}$ *Nlrp3*$^{-/-}$ DKO, $n = 7$; for cGAMP followed by saline: $n = 6$ for all strains. Error bars, SEM; ns, not significant; *, $P < 0.05$; ****, $P < 0.0001$.

cells caused a dramatic reduction in IL-1β secretion at all three time points (Fig. 8 b). This indicates that cGAS is required for IL-1β production in an IFN-independent fashion during MCMV infection. We next assayed MCMV genome copy number by qPCR to determine whether both arms of cGAMP signaling are required for optimal control of the viral genome. 2 d after MCMV infection, MCMV genome copy number increased significantly in both *Ifnar*$^{-/-}$ and *Ifnar*$^{-/-}$ *cGAS*$^{-/-}$ DKO BMDMs compared with WT (Fig. 8 c). Importantly, MCMV genome copy in *Ifnar*$^{-/-}$ *cGAS*$^{-/-}$ DKO cells was significantly increased compared with *Ifnar*$^{-/-}$, supporting a role for cGAS in controlling MCMV that is independent of its IFN-I signaling.

The aforementioned data indicate that during MCMV infection, cGAS/cGAMP activity other than IFN-I signaling was important for the control of viral genome copy. We next investigated whether inflammasome activation was the other activity necessary for MCMV genome copy control. To address this, WT and *Ifnar*$^{-/-}$ BMDMs were infected with MCMV in the presence or absence of the caspase-1 inhibitor, Z-YVAD. Fig. 8 d shows that Z-YVAD inhibited MCMV-induced inflammasome activity to similar levels in WT and *Ifnar*$^{-/-}$ BMDMs. MCMV genome copy was significantly increased in WT with Z-YVAD BMDMs compared with WT alone (Fig. 8 e, left), suggesting a role for inflammasome in control of the viral genome. Within the same experiment, MCMV genome copy number was significantly increased in *Ifnar*$^{-/-}$ BMDMs, and this was further augmented when caspase-1 was inhibited by the addition of Z-YVAD (Fig. 8 e, right). This suggests that both IFN-I signaling and inflammasome activation are important for MCMV genome copy control. Collectively, these data show that during MCMV infection, cGAS is important for inflammasome activation.

MCMV infection in vivo is known to be dependent on IFN-I signaling, mostly induced through STING, and also dependent on IFNγ (Lio et al., 2016). IL-18, an inflammasome-activated cytokine, is a known inducer of IFNγ. Because of this, we investigated whether both arms of cGAS downstream signaling, IFN-I production and inflammasome activation, are necessary for control of in vivo MCMV infection in mice. WT, *Ifnar*$^{-/-}$, and *Ifnar*$^{-/-}$ *cGAS*$^{-/-}$ DKO mice were infected with $10^5$ pfu MCMV. After 36 h, levels of IL-18, as a measure of inflammasome activation, and IFNγ were quantified. Serum IL-18 levels were not different between WT and *Ifnar*$^{-/-}$ mice after MCMV infection, confirming our in vitro data showing that inflammasome activation is not dependent on IFN-I (Fig. 8 f). MCMV-infected *Ifnar*$^{-/-}$ *cGAS*$^{-/-}$ DKO mice, however, had significantly less IL-18 serum levels than *Ifnar*$^{-/-}$ mice (Fig. 8 f). This strongly suggests that cGAS has a role in inflammasome activation independent of its IFN-I signaling arm. IFNγ was also significantly decreased in MCMV-infected *Ifnar*$^{-/-}$ *cGAS*$^{-/-}$ DKO mice compared with *Ifnar*$^{-/-}$ mice (Fig. 8 g). This suggests that cGAS stimulation plays a role in IFNγ production during early MCMV infection, independently of IFN-I signaling. We next determined viral genome numbers for spleens of infected mice. Both *Ifnar*$^{-/-}$ and *Ifnar*$^{-/-}$ *cGAS*$^{-/-}$ DKO mice had significantly more viral genome copies in their spleens than WT mice (Fig. 8 h). Importantly viral genome copies for MCMV-infected *Ifnar*$^{-/-}$ *cGAS*$^{-/-}$ DKO mice were significantly more numerous than *Ifnar*$^{-/-}$ mice (Fig. 8 h). These data strongly suggest that cGAS's role in controlling MCMV infection is twofold. The first is well known: the production of IFN-β that acts to limit the spread of the infection. The second is in the activation of inflammasome.

## DISCUSSION

Recognition of pathogen DNA occurs by multiple DNA sensors, located in various host compartments. Many of these DNA sensors trigger the IFN-I pathway, which is crucial in limiting and clearing many viral and microbial infections (Wilkins and Gale, 2010; Dempsey and Bowie, 2015). Although the intracellular DNA sensor, cGAS, is widely expressed in most cell types, a seminal discovery is that it represents the major sensor of DNA for the induction of the IFN-I pathway in immune cells (Sun et al., 2013; Wu et al., 2013). cGAS exerts its power by the production of the second

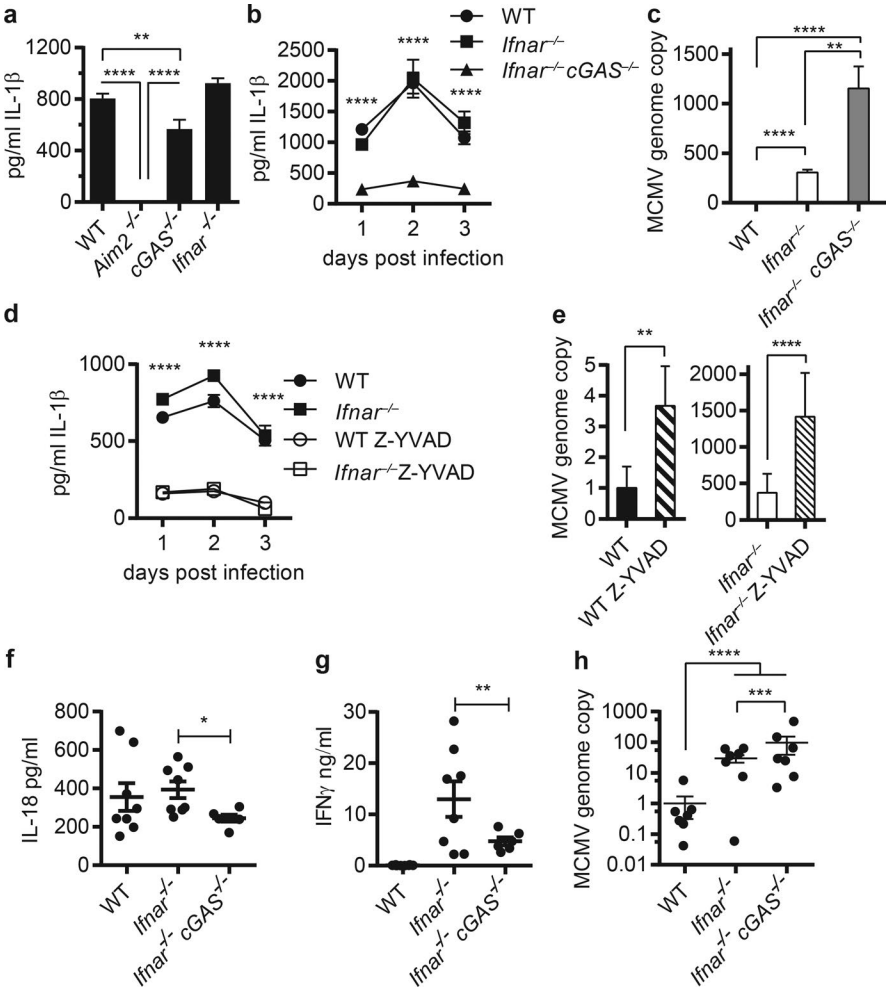


Figure 8. **cGAS-dependent inflammasome activation is necessary for the control of MCMV.** WT, *Aim2*$^{-/-}$, *cGAS*$^{-/-}$, or *Ifnar*$^{-/-}$ BMDMs were infected with MCMV at multiplicity of infection 1. (a) IL-1β ELISA of supernatants from BMDMs 1 d postinfection. (b and c) WT, *Ifnar*$^{-/-}$, or *Ifnar*$^{-/-}$*cGAS*$^{-/-}$ BMDMs were infected with MCMV at multiplicity of infection 1. (b) IL-1β ELISA of supernatants from BMDMs 1–3 d postinfection. (c) Relative MCMV genome copy number from BMDMs 2 d postinfection. (d and e) WT and *Ifnar*$^{-/-}$ BMDMs were infected in the presence or absence of caspase-1 inhibitor, Z-YVAD, and assayed for IL-1β (d) or relative MCVM genome copy (e). In e, left and right panels are from the same experiment. $n = 2$ independent experiments. Shown is a representative experiment with technical replicates of six; mean ± SEM. (f and g) WT, *Ifnar*$^{-/-}$, or *Ifnar*$^{-/-}$ *cGAS*$^{-/-}$ mice were infected with MCMV for 36 h. IL-18 serum levels (f), IFNγ spleen levels (g), and relative MCMV genome copy number from spleens after infection (h). $n = 8$. Error bars, SEM; *, $P < 0.05$; **, $P < 0.01$; ***, $P < 0.001$; ****, $P < 0.0001$.

messenger 2′3′-cGAMP after binding to DNA. 2′3′-cGAMP then binds to STING, leading to the production of IFN-β.

AIM2, another DNA sensor, belongs to the IFI16/HIN200 family of DNA sensors. It was initially found to be a tumor suppressor and induce cell cycle arrest (DeYoung et al., 1997; Patsos et al., 2010). It has more recently been found to regulate colon cancer tumorigenesis through suppression of AKT, a regulator of cellular proliferation (Wilson et al., 2015). In addition to its role as a tumor suppressor, AIM2 was found to sense DNA in the cytosol and induce the formation of an inflammasome for the secretion of IL-1β and IL-18 and induction of pyroptosis (Bürckstümmer et al., 2009; Fernandes-Alnemri et al., 2009; Hornung et al., 2009; Roberts et al., 2009).

Sensing of pathogen DNA during infection by multiple sensors enables the cells to respond with a larger repertoire of cytokines. The two cytoplasmic DNA sensors, cGAS and AIM2, have been thought to initiate two separate outcomes with regard to cytokine production, IFN-I signaling and inflammasome activation, respectively, and work independently of each other. The work presented here suggests otherwise: that the two innate pathways are intricately linked via the second messenger, 2′3′-cGAMP. The use of a second messenger provides cytosolic DNA sensing via cGAS an opportunity for bifurcation to activate two important innate immune pathways.

How the Aim2 inflammasome is activated and its importance in many pathogenic infections is well known (Rathinam et al., 2010). We have shown here the importance of the second messenger 2′3′-cGAMP for the full activation of the Aim2 inflammasome during dAdT-DNA sensing and during MCMV infection. Although it is unexpected that a cell would have cytosolic 2′3′-cGAMP without also finding cytosolic DNA present, we have been able to discern the role of cGAMP in enhancing the DNA-induced Aim2 inflammasome using knockout mice and transfection of cGAMP without additional DNA. We show that the cGAMP-induced inflammasome is dependent on Aim2, Nlrp3, and Asc and uses the canonical caspase-1.

Activation of the inflammasome is considered a two-step process, with the first step of up-regulating inflammasome components and the second step of activating the inflammasome. The priming step of inflammasomes in general has been shown to occur via IFN-I, NF-κB, and TNF signaling. Pathogen infection of cells is known to activate these signal-

ing pathways through engagement of a variety of intracellular and extracellular receptors, including the TLRs, NLRs, ALRs, and RLRs, so that it is expected that during a pathogenic infection priming of the inflammasome would occur. Using LPS to prime BMDMs, our data show that Sting is not required for inflammasome priming of inflammasome component transcription, although it is needed for full activation of the cGAMP-induced inflammasome.

DNA is known to be able to self-prime and activate the Aim2 inflammasome without a separate priming step, albeit with slower kinetics. cGAMP activation of IFN-I occurred earlier, whereas its activation of IL-1β secretion took place after IFN-I subsided; thus the two cytokines may regulate immune response in tandem. We found that cGAMP activation of the Aim2 inflammasome is similar in its ability to self-prime and activate the Aim2 inflammasome. We show that cGAMP primes the inflammasome through its IFN-β production, leading to IFN-I signaling, as priming of all inflammasome components was abolished in *Ifnar*$^{-/-}$ and *Sting*-deficient BMDMs. This is interesting because cGAMP binding to Sting also activates NF-κB and TNF, signaling pathways known to prime inflammasome components.

An important finding from our data is the observation that both cGAS-dependent inflammasome activation and IFN-I signaling are crucial for the control of the MCMV viral genome. Although independently IFN-I and inflammasome contribute to impart antiviral effects, together the coordinated actions of cGAS/cGAMP amplify their effects. Thus the capacity of cGAS/cGAMP to enhance inflammasome and IFN-I is central to the function of the DNA sensor cGAS.

Although a previous study showed that the bacterial CDNs c-di-GMP and c-di-AMP induced inflammasome activation, with c-di-GMP being more efficient than c-di-AMP (Abdul-Sater et al., 2013), this work shows that c-di-GMP is significantly less efficient in inflammasome activation than the canonical 2′3′-cGAMP. Additionally, our data show that cGAMP activates the inflammasome via an AIM2-NLRP3-ASC–dependent pathway, which differs from bacterial-derived c-di-GMP, which goes through an NLRP3 pathway. Furthermore, the previous work did not assess whether the c-di-GMP–induced inflammasome was important in physiological settings, including during microbial infection or in animals. This work shows that cGAMP-induced inflammasome activation enhances DNA-induced inflammasome to its full potential for the control of MCMV. One rare feature of the cGAMP-induced inflammasome is that it heightens cytokine secretion without altering pyroptosis. Lack of inflammasome-dependent cell death has only recently been shown during induction of the noncanonical caspase-11 inflammasome by oxidized phospholipids, and is specific for DCs (Zanoni et al., 2016). It is noteworthy that unlike c-di-GMP and c-di-AMP, which are produced by bacteria, cGAMP is a self-molecule and has roles in both infection and autoimmunity. Thus our findings are relevant to a wide range of disorders beyond pathogen infection.

Recently, there have been studies suggesting that inflammasome activation can occur through two sensors to work in concert with each other (Kim et al., 2010, 2015; Wu et al., 2010; Kayagaki et al., 2011; Kalantari et al., 2014; Man et al., 2014; Zhao et al., 2014; Denes et al., 2015; Karki et al., 2015; Vance, 2015; Qu et al., 2016). Our work shows directly by confocal microscopy that AIM2, NLRP3, and ASC form a single focus within cells to activate DNA-induced inflammasome. Exactly how AIM2 and NLRP3 work together during inflammasome activation is currently unclear. For AIM2 and NLRP3 inflammasomes, it has been shown that stimulation by their corresponding PAMPs or DAMPs induces ring-like septamer formation of the sensor that acts to nucleate ASC oligomerization at their pyrin domains (Lu et al., 2014). In the case of AIM2 and NLRP3 multi-effector complexes, it may be that each effector activates individual inflammasome units that aggregate together either upon polymerized ASC or alternatively by their effector domains, as suggested for NLRC4 and NLRP3 (Qu et al., 2016), shown in the model (Fig. 4 a). Another possibility, although less likely, is that the individual inflammasome septamer-sensor units that initially form are composed of a mixture of effector molecules, for instance AIM2 and NLRP3. For this model, if the sensors are able to hetero-oligomerize, size differences between the two effectors likely would make it difficult for the pyrin domains to accurately align for ASC polymerization to occur.

In summary, recognition of PAMPs and DAMPs by host cells is vital in mounting an immune response to pathogens. Coordination of this response is crucial to fighting and overcoming infection. Because viruses, bacteria, and fungi all present the cell with multiple PAMPs, the host must coordinate its multipronged response and refine it to fight the infection without deleterious outcomes for the host. Our work heightens the understanding of cytosolic DNA sensing. Although the use of second messengers is known to amplify downstream signaling, the second messenger cGAMP provides two functions. The canonical function, which is well documented, indicates that it engages STING to amplify IFN-I signaling; the noncanonical function is induction of inflammasome formation and enhancement of DNA-induced inflammasomes. Together, our data suggest that cGAMP is one of the mechanisms by which host cells coordinate their attack by linking IFN-I signaling and inflammasome activation.

## MATERIALS AND METHODS

### Experimental animals

*Asc*$^{-/-}$, *Aim2*$^{-/-}$, *Nlrp3*$^{-/-}$, *Nlrc4*$^{-/-}$, *Ice*$^{-/-}$ (*Casp1*$^{-/-}$ *Casp11*$^{129mt/129mt}$), *Casp1*$^{-/-}$ (*Ice*$^{-/-}$ *Casp11*$^{tg}$), and *Casp11*$^{-/-}$ mice on the C57BL/6 background have been described elsewhere (Mariathasan et al., 2004; Sutterwala et al., 2006; Broz et al., 2010; Kayagaki et al., 2011; Wilson et al., 2015). *Casp1*$^{-/-}$ and *Casp11*$^{-/-}$ mice were provided by V.M. Dixit at Genentech (South San Francisco, CA). *Ifnar*$^{-/-}$ and *Sting*$^{gt/gt}$ mice on the C57BL/6 background and were purchased from Jackson Laboratory (028288 and 017537, respectively). The

cGAS KO mice (*Mb21d1*$^{-/-}$ or *cGAS*$^{-/-}$) were generated by crossing *Mb21d1*$^{tm1a(EUCOMM)Hmgu}$ mice containing the *cGAS* targeting vector on the C57BL/6 background (International Mouse Phenotyping Consortium) to mice expressing FLPe recombinase under the control of the *Gt(ROSA)26Sor* promoter (016226; Jackson Laboratory) to excise the *lacZ* and neomycin cassettes, leaving exon 2 floxed. The conditional mutant mice were then bred to mice expressing Cre under the control of the actin promoter (019099; Jackson Laboratory) mice to excise exon 2. Mice were backcrossed with WT C57BL/6J for three generations to remove *FLPe* and *cre* transgenes. WT C57BL/6J mice were obtained from Jackson Laboratory and maintained at University of North Carolina Chapel Hill for more than nine generations. All animal protocols were approved by the University of North Carolina Chapel Hill Institutional Animal Care and Use Committee in accordance with the National Institutes of Health Guide for the Care and Use of Laboratory Animals. Animal numbers were empirically determined to optimize numbers necessary for statistical significance (minimum of five to eight animals/group for each type of analysis). All in vivo experiments were performed under specific pathogen–free conditions using 6–8-wk-old female mice. No randomization of animals was used.

Mice were intranasally dosed with 30 µl saline or 5 mg/ml 2′3′-cGAMP in saline (InvivoGen). After 24 h, the mice received a second dose of either saline or cGAMP. 4 h after the second dose, BALF was collected in 1 ml HBSS with 3 mM EDTA. Bronchial lavage cells were cytospun onto slides and stained with Diff-Quick (Siemens Healthcare Diagnostics), and macrophages were counted by a trained pathologist blinded to the experimental conditions of the study.

### Cell culture

BMDMs were prepared by flushing femurs of 6–12-wk-old age-matched male mice. RBCs were lysed with ACK lysis buffer (Gibco), and the progenitor cells were differentiated in DMEM with 30% L29 conditioned media with 20% FBS for 6–7 d. Progenitor cells were differentiated into BMDCs in RPMI 1640 with 10% FBS and 40 ng/ml GM-CSF (Peprotech) for 8–9 d. Mouse DC line JAWSII (CRL-11904; ATCC) was grown in DMEM with NTPs, 20% FBS, and 10 ng/ml GM-CSF. JAWSII cells were infected with lentivirus containing AIM2-Flag under the doxycycline promoter and selected for integration with puromycin (Wilson et al., 2015). Lentivirus vector containing sh-cGAS was purchased from Open Biosystems and used to make lentivirus stock. JAWSII cells were infected with sh-cGAS lentivirus and selected with G418. Human DCs were provided to us by J.S. Serody (Dees et al., 2004). The cells were isolated from patients enrolled in a study approved by the University of North Carolina Institutional Review Board after providing written informed consent. Human DCs were provided to us frozen from day 9–12 CD34$^{+}$ cells differentiated to DCs. After the cells were thawed, they were grown in AIM V medium (Gibco) with 10% human AB serum (Gemcell) containing GM-CSF (800 U/ml; Leukine, Genzyme Corporation) and IL-4 (500 U/ml; Peprotech). Human macrophages were differentiated from human peripheral blood monocytes (PBMCs) that were isolated from leukapheresis buffy coat (Gulf Coast Regional Blood Center) by separation of cells over a lymphoprep density gradient following the manufacturer's protocol (StemCell Technologies). PBMCs were suspended in AIM V medium with 10% human serum and allowed to attach to T75 flasks for 2 h. Unattached cells were gently washed off, and the remaining adherent PBMCs were incubated in AIMV media with 10% human serum with 800 U/ml GM-CSF at 37 in 5% $CO_2$ for 3 d.

### MCMV infection

Construction and production of MCMV-GFP has been described previously (Mathys et al., 2003; Benedict et al., 2008). BMDM and JAWS II DCs were activated with 200 ng/ml LPS for 2 h before infecting with MCMV-GFP at multiplicity of infection 1. Anti–IFN-β neutralizing polyclonal antibody (PBL, 32400-1, lot #5792) was used at $2 \times 10^4$ NU/ml and added immediately before MCMV infection. Caspase-1 inhibitor, Z-YVAD (sc-3071; Santa Cruz Biotechnology) was used at 20 µM and added with the MCMV. Mice were infected intraperitoneally with $1 \times 10^5$ pfu. Spleens and serum were collected 36 h postinfection.

### Reagents

Mouse IL-1β was measured using the OptEIA kit (559603; BD Biosciences), IL-18 was measured with IL-18 platinum ELISA (BMS618/2TEN; eBioscience), Tnf was measured by ELISA (558534; BD Biosciences), IFNγ was detected by ELISA (430802; BioLegend), and IFN-β was measured by coating plates with capture anti-IFN-β (clone 75-D3; Santa Cruz Biotechnology) and using detection rabbit polyclonal anti-IFN-β (32400-1; PBL). Human IL-1β was detected with the OptEIA kit set II (557953; BD Biosciences). Ultrapure LPS, 2′3′-cGAMP, 3′3′-cGAMP, c-di-GMP, dAdT, ATP, and nigericin were purchased from InvivoGen. Cell death was determined with use of ToxiLight cytotoxicity bioassay (Lonza) that measures release of adenylate cyclase, following the manufacturer's instructions.

### Inflammasome assays

Cells were plated at $2 \times 10^5$ cells per well of a 24-well dish in DMEM with 10% FBS the night before the assay. The next morning, cells were washed once in PBS, and 250 µl DMEM and 10% FBS with 200 ng/ml ultrapure LPS was added for 3 h to prime the cells in some cases. 5 or 10 nM of the CDNs were transfected with Lipofectamine RNAiMax (1.5 µl/reaction) or Lipofectamine 2000 (1 µl/reaction; Invitrogen), and 1 µg/ml dAdT was transfected with Lipofectamine 2000 (Invitrogen) in OptiMem (Invitrogen) into the cells, with lesser amounts noted in the figure legends and text. Nigericin was added at 2 µM, and

ATP was added at 5 mM. Supernatants were collect 6 h after stimulation for LPS-primed cells or 19 h poststimulation with no LPS priming. The use of Lipofectamine RNAiMax proved to transfect cGAMP more efficiently, with less cell death, and with less background IL-1β induction in the transfection-only controls, than Lipofectamine 2000.

### qPCR

After stimulation of cells, total RNA was extracted from cells with RNAeasy Plus mini kit (Qiagen), and cDNA was generated with iSCRIPT (170-8841; Bio-Rad) according to the manufacturers' instructions. Real-time PCR was performed with mouse *Il1b* (Mm01336189), *Asc* (Mm00445747), *Mb21d1* (*cGAS*, Mm01147496 and Mm01147497), *Casp1* (Mm00438023), *Aim2* (m01295719), *Nlrp3* (Mm00840904), and *Ifnb1* (Mm00439546) gene expression using mouse Taqman gene expression assays (Applied Biosystems). The results were normalized against *Rps13* (Mm00850011) and *Gapdh* and cycled on a ViiA7 Real-Time thermocycler (Life Technologies). Amounts were quantified by the ΔΔCT method with use of ViiA7 software. Statistical analysis was done with ViiA7 software. To quantify MCMV genome copies, DNA was collected by washing the cells twice with DMEM before lysing the cells in 50 mM NaOH for 10–15 min at 37°C. Lysates were neutralized in 3 V of 37 mM Tris, pH 8.0. MCMV genomes were detected using three separate primer sets for *ie1* and normalized against *Asc*: IE1-1F, 5′-CTCACAGCAACT CATCCTATCC-3′; IE1-1R, 5′-GGGTCACCTCATCAT CATCTTC-3′; IE1-2F, 5′-AGAGTCCCTTCACCAAGA AATG-3′; IE1-2R, 5′-GGCTGCACAGGTGAGATAAA-3′; IE1-3F, 5′-CTGCCTGTCTATCCCTATCTATCT-3′; IE1-3R, 5′-CCATCACCAGCGTTCTACTT-3′; ASC-1F, 5′-CGCCATAGATCTCACTGACAAA-3′; ASC-1R, 5′-TCCTGTAAGCCCATGTCTCTA-3′; ASC-2F, 5′-GGAAAGAACAGGAGCTGTAAGA-3′; and ASC-2R, 5′-GCCAAGACCAGGAAGTCAG-3′.

### Immunoblotting

After stimulation, cells were washed once in PBS and lysed directly in SDS-PAGE gel loading buffer. Supernatants were diluted 1:1 in the same buffer. Samples were separated through 4–15% TGX precast gels (Bio-Rad) and transferred to nitrocellulose. The nitrocellulose blots were blocked with 5% nonfat dry milk and incubated overnight with antibodies against IL-1β (AB-401-NA; R&D Systems), caspase-1 (AG-20B-0042; Adipogen), Nlrp3 (AG-20B-0014; Adipogen), and Sting (50494; Cell Signaling Technology).

### Confocal microscopy

Cells were seeded onto glass coverslips in 24-well dishes and processed as for inflammasome assays. For JAWSII cells expressing AIM2-Flag, cells were exposed to 10 μg/ml doxycycline during the 3-h LPS priming step. The doxycycline was removed with three PBS washes, and 200 ng/ml LPS in DMEM/10% FBS was added to the cells, before transfection of the cells with cGAMP for 3 h. For cGAMP-only assays, unlabeled cGAMP was mixed with cGAMP-fluorescein (C 178-001; Biolog) in a 30:1 ratio; for assays with dAdT and cGAMP, 160 pmol cGAMP-fluorescein was mixed with 0.5 μg dAdT-rhodamine (InvivoGen) and transfected with Lipofectamine 2000. The cells were fixed in 4% PFA before staining. When used, active caspase-1 was visualized by the addition of FLICA-660 caspase-1 assay kit (9122; ImmunoChemistry Technologies) for the final hour during the transfection, following the manufacturer's protocol. Cells were permeabilized with 0.05% saponin in DMEM/10% FBS. Antibodies to Flag (clone M2, F1894; Sigma-Aldrich), NLRP3 (AG-20B-0014-C100; Adipogen), and Asc (ADI-905-173-100; Enzo Life Sciences) were diluted in permeabilization solution and incubated with the cells for 1 h, washed three times in permeabilization solution, and incubated with anti–rabbit IgG AF-405 (ASC), anti–mouse IgG1 AF-633 (Aim2-Flag), and anti–mouse IgG2b AF-546 (Nlrp3) when cells were transfected with cGAMP alone, or mouse anti-IgG AF-405 (AIM2-Flag) when cells were transfected with cGAMP and dAdT. Cells were imaged on a Zeiss 700 confocal microscope. Overlap coefficient and Pearson's coefficient were determined using ImageJ software on individual confocal slices. Pearson's coefficient ranges from 1 (highly colocalized) to −1 (highly excluded) and takes into account intensity of the pixels. The overlap coefficient ranges from 1 (highly colocalized) to 0 (low colocalization) and does not consider intensity of pixels.

### Statistical analysis

Results are presented as the mean ± SEM for experiments with $n \geq 3$. Results are presented as the mean ± SD for individual human donors and qPCR. Significance between two groups was assessed by Student's two-tailed *t* test. Datasets consisting of more than two groups were analyzed by analysis of variance with Tukey–Kramer honestly significant difference posttest for multiple comparisons if significance was determined. A *p*-value that was less than 0.05 was considered statistically significant for all datasets. All statistical analysis was performed using GraphPad Prism software except for qPCR data. Statistical analysis for qPCR was done with ViiA7 software. A single sample (WT mouse from Fig. 7 b) was excluded as an outlier for being greater than 3 SD from the mean.

### Online supplemental material

Fig. S1 shows Nlrp3 stressors that cGAMP induces for inflammasome activation. Fig. S2 shows confocal analysis of cGAMP- or DNA-induced inflammasomes. Fig. S3 shows bronchiolar macrophage cell count after in vivo cGAMP administration.

## ACKNOWLEDGMENTS

We acknowledge the Microscopy Services Laboratory within the UNC Core Services, where all confocal microscopy experiments were performed.

This work is supported by the U.S. National Institutes of Health (NIH) U19 AI109965, AI067798, U19 AI109784, and R37 AI029564 to J.P.-Y. Ting; NIH RO1 AI101423 to C.A. Benedict; NIH T32 AI007151 to R.D. Junkins; NIH T32 AI07273 to C.J. Kurkjian; and NIH T32 CA009156 and American Cancer Society PF-15-047-01-MPC to A.A. Pendse.

The authors declare no competing financial interests.

Author contributions: K.V. Swanson designed and conducted the experiments. R.D. Junkins performed the in vivo MCMV infections. C.J. Kurkjian, E. Holley-Guthrie, A.A. Pendse, R. El Morabiti and A. Petrucelli assisted with the experiments. G.N. Barber and C.A. Benedict provided intellectual input and/or reagents. J.P.-Y. Ting supervised the project. K.V. Swanson and J.P.-Y. Ting interpreted the data and wrote the manuscript.

**Submitted: 20 September 2017**

**Revised: 3 October 2017**

**Accepted: 4 October 2017**

## REFERENCES

Aachoui, Y., I.A. Leaf, J.A. Hagar, M.F. Fontana, C.G. Campos, D.E. Zak, M.H. Tan, P.A. Cotter, R.E. Vance, A. Aderem, and E.A. Miao. 2013. Caspase-11 protects against bacteria that escape the vacuole. *Science.* 339:975–978. https://doi.org/10.1126/science.1230751

Abdul-Sater, A.A., I. Tattoli, L. Jin, A. Grajkowski, A. Levi, B.H. Koller, I.C. Allen, S.L. Beaucage, K.A. Fitzgerald, J.P. Ting, et al. 2013. Cyclic-di-GMP and cyclic-di-AMP activate the NLRP3 inflammasome. *EMBO Rep.* 14:900–906. https://doi.org/10.1038/embor.2013.132

Ahn, J., D. Gutman, S. Saijo, and G.N. Barber. 2012. STING manifests self DNA-dependent inflammatory disease. *Proc. Natl. Acad. Sci. USA.* 109:19386–19391. https://doi.org/10.1073/pnas.1215006109

Barber, G.N. 2014. STING-dependent cytosolic DNA sensing pathways. *Trends Immunol.* 35:88–93. https://doi.org/10.1016/j.it.2013.10.010

Bauernfeind, F.G., G. Horvath, A. Stutz, E.S. Alnemri, K. MacDonald, D. Speert, T. Fernandes-Alnemri, J. Wu, B.G. Monks, K.A. Fitzgerald, et al. 2009. Cutting edge: NF-kappaB activating pattern recognition and cytokine receptors license NLRP3 inflammasome activation by regulating NLRP3 expression. *J. Immunol.* 183:787–791. https://doi.org/10.4049/jimmunol.0901363

Benedict, C.A., A. Loewendorf, Z. Garcia, B.R. Blazar, and E.M. Janssen. 2008. Dendritic cell programming by cytomegalovirus stunts naive T cell responses via the PD-L1/PD-1 pathway. *J. Immunol.* 180:4836–4847. https://doi.org/10.4049/jimmunol.180.7.4836

Bhat, N., and K.A. Fitzgerald. 2014. Recognition of cytosolic DNA by cGAS and other STING-dependent sensors. *Eur. J. Immunol.* 44:634–640. https://doi.org/10.1002/eji.201344127

Broz, P., and V.M. Dixit. 2016. Inflammasomes: Mechanism of assembly, regulation and signalling. *Nat. Rev. Immunol.* 16:407–420. https://doi.org/10.1038/nri.2016.58

Broz, P., K. Newton, M. Lamkanfi, S. Mariathasan, V.M. Dixit, and D.M. Monack. 2010. Redundant roles for inflammasome receptors NLRP3 and NLRC4 in host defense against *Salmonella*. *J. Exp. Med.* 207:1745–1755. https://doi.org/10.1084/jem.20100257

Bürckstümmer, T., C. Baumann, S. Blüml, E. Dixit, G. Dürnberger, H. Jahn, M. Planyavsky, M. Bilban, J. Colinge, K.L. Bennett, and G. Superti-Furga. 2009. An orthogonal proteomic-genomic screen identifies AIM2 as a cytoplasmic DNA sensor for the inflammasome. *Nat. Immunol.* 10:266–272. https://doi.org/10.1038/ni.1702

Cai, X., J. Chen, H. Xu, S. Liu, Q.X. Jiang, R. Halfmann, and Z.J. Chen. 2014a. Prion-like polymerization underlies signal transduction in antiviral immune defense and inflammasome activation. *Cell.* 156:1207–1222. https://doi.org/10.1016/j.cell.2014.01.063

Cai, X., Y.H. Chiu, and Z.J. Chen. 2014b. The cGAS-cGAMP-STING pathway of cytosolic DNA sensing and signaling. *Mol. Cell.* 54:289–296. https://doi.org/10.1016/j.molcel.2014.03.040

Dees, E.C., K.P. McKinnon, J.J. Kuhns, K.A. Chwastiak, S. Sparks, M. Myers, E.J. Collins, J.A. Frelinger, H. Van Deventer, F. Collichio, et al. 2004. Dendritic cells can be rapidly expanded ex vivo and safely administered in patients with metastatic breast cancer. *Cancer Immunol. Immunother.* 53:777–785. https://doi.org/10.1007/s00262-004-0520-1

Dempsey, A., and A.G. Bowie. 2015. Innate immune recognition of DNA: A recent history. *Virology.* 479-480:146–152. https://doi.org/10.1016/j.virol.2015.03.013

Denes, A., G. Coutts, N. Lénárt, S.M. Cruickshank, P. Pelegrin, J. Skinner, N. Rothwell, S.M. Allan, and D. Brough. 2015. AIM2 and NLRC4 inflammasomes contribute with ASC to acute brain injury independently of NLRP3. *Proc. Natl. Acad. Sci. USA.* 112:4050–4055. https://doi.org/10.1073/pnas.1419090112

DeYoung, K.L., M.E. Ray, Y.A. Su, S.L. Anzick, R.W. Johnstone, J.A. Trapani, P.S. Meltzer, and J.M. Trent. 1997. Cloning a novel member of the human interferon-inducible gene family associated with control of tumorigenicity in a model of human melanoma. *Oncogene.* 15:453–457. https://doi.org/10.1038/sj.onc.1201206

Fernandes-Alnemri, T., J.W. Yu, P. Datta, J. Wu, and E.S. Alnemri. 2009. AIM2 activates the inflammasome and cell death in response to cytoplasmic DNA. *Nature.* 458:509–513. https://doi.org/10.1038/nature07710

Guarda, G., M. Braun, F. Staehli, A. Tardivel, C. Mattmann, I. Förster, M. Farlik, T. Decker, R.A. Du Pasquier, P. Romero, and J. Tschopp. 2011. Type I interferon inhibits interleukin-1 production and inflammasome activation. *Immunity.* 34:213–223. https://doi.org/10.1016/j.immuni.2011.02.006

Guo, H., J.B. Callaway, and J.P. Ting. 2015. Inflammasomes: Mechanism of action, role in disease, and therapeutics. *Nat. Med.* 21:677–687. https://doi.org/10.1038/nm.3893

He, Y., and A.O. Amer. 2014. Microbial modulation of host apoptosis and pyroptosis. *Front. Cell. Infect. Microbiol.* 4:83. https://doi.org/10.3389/fcimb.2014.00083

Hornung, V., A. Ablasser, M. Charrel-Dennis, F. Bauernfeind, G. Horvath, D.R. Caffrey, E. Latz, and K.A. Fitzgerald. 2009. AIM2 recognizes cytosolic dsDNA and forms a caspase-1-activating inflammasome with ASC. *Nature.* 458:514–518. https://doi.org/10.1038/nature07725

Ishikawa, H., and G.N. Barber. 2008. STING is an endoplasmic reticulum adaptor that facilitates innate immune signalling. *Nature.* 455:674–678. https://doi.org/10.1038/nature07317

Jin, L., P.M. Waterman, K.R. Jonscher, C.M. Short, N.A. Reisdorph, and J.C. Cambier. 2008. MPYS, a novel membrane tetraspanner, is associated with major histocompatibility complex class II and mediates transduction of apoptotic signals. *Mol. Cell. Biol.* 28:5014–5026. https://doi.org/10.1128/MCB.00640-08

Jin, T., A. Perry, J. Jiang, P. Smith, J.A. Curry, L. Unterholzner, Z. Jiang, G. Horvath, V.A. Rathinam, R.W. Johnstone, et al. 2012. Structures of the HIN domain:DNA complexes reveal ligand binding and activation mechanisms of the AIM2 inflammasome and IFI16 receptor. *Immunity.* 36:561–571. https://doi.org/10.1016/j.immuni.2012.02.014

Kalantari, P., R.B. DeOliveira, J. Chan, Y. Corbett, V. Rathinam, A. Stutz, E. Latz, R.T. Gazzinelli, D.T. Golenbock, and K.A. Fitzgerald. 2014. Dual engagement of the NLRP3 and AIM2 inflammasomes by plasmodium-derived hemozoin and DNA during malaria. *Cell Reports.* 6:196–210. https://doi.org/10.1016/j.celrep.2013.12.014

Karki, R., S.M. Man, R.K. Malireddi, P. Gurung, P. Vogel, M. Lamkanfi, and T.D. Kanneganti. 2015. Concerted activation of the AIM2 and NLRP3 inflammasomes orchestrates host protection against Aspergillus infection. *Cell Host Microbe.* 17:357–368. https://doi.org/10.1016/j.chom.2015.01.006

Kayagaki, N., S. Warming, M. Lamkanfi, L. Vande Walle, S. Louie, J. Dong, K. Newton, Y. Qu, J. Liu, S. Heldens, et al. 2011. Non-canonical inflammasome activation targets caspase-11. *Nature.* 479:117–121. https://doi.org/10.1038/nature10558

Kim, H.Y., S.J. Kim, and S.M. Lee. 2015. Activation of NLRP3 and AIM2 inflammasomes in Kupffer cells in hepatic ischemia/reperfusion. *FEBS J.* 282:259–270. https://doi.org/10.1111/febs.13123

Kim, S., F. Bauernfeind, A. Ablasser, G. Hartmann, K.A. Fitzgerald, E. Latz, and V. Hornung. 2010. Listeria monocytogenes is sensed by the NLRP3 and AIM2 inflammasome. *Eur. J. Immunol.* 40:1545–1551. https://doi.org/10.1002/eji.201040425

Laudisi, F., R. Spreafico, M. Evrard, T.R. Hughes, B. Mandriani, M. Kandasamy, B.P. Morgan, B. Sivasankar, and A. Mortellaro. 2013. Cutting edge: the NLRP3 inflammasome links complement-mediated inflammation and IL-1β release. *J. Immunol.* 191:1006–1010. https://doi.org/10.4049/jimmunol.1300489

Lio, C.W., B. McDonald, M. Takahashi, R. Dhanwani, N. Sharma, J. Huang, E. Pham, C.A. Benedict, and S. Sharma. 2016. cGAS-STING signaling regulates initial innate control of cytomegalovirus infection. *J. Virol.* 90:7789–7797. https://doi.org/10.1128/JVI.01040-16

Lu, A., V.G. Magupalli, J. Ruan, Q. Yin, M.K. Atianand, M.R. Vos, G.F. Schröder, K.A. Fitzgerald, H. Wu, and E.H. Egelman. 2014. Unified polymerization mechanism for the assembly of ASC-dependent inflammasomes. *Cell.* 156:1193–1206. https://doi.org/10.1016/j.cell.2014.02.008

Malireddi, R.K., and T.D. Kanneganti. 2013. Role of type I interferons in inflammasome activation, cell death, and disease during microbial infection. *Front. Cell. Infect. Microbiol.* 3:77. https://doi.org/10.3389/fcimb.2013.00077

Man, S.M., L.J. Hopkins, E. Nugent, S. Cox, I.M. Glück, P. Tourlomousis, J.A. Wright, P. Cicuta, T.P. Monie, and C.E. Bryant. 2014. Inflammasome activation causes dual recruitment of NLRC4 and NLRP3 to the same macromolecular complex. *Proc. Natl. Acad. Sci. USA.* 111:7403–7408. https://doi.org/10.1073/pnas.1402911111

Mariathasan, S., K. Newton, D.M. Monack, D. Vucic, D.M. French, W.P. Lee, M. Roose-Girma, S. Erickson, and V.M. Dixit. 2004. Differential activation of the inflammasome by caspase-1 adaptors ASC and Ipaf. *Nature.* 430:213–218. https://doi.org/10.1038/nature02664

Martinon, F., K. Burns, and J. Tschopp. 2002. The inflammasome: A molecular platform triggering activation of inflammatory caspases and processing of proIL-beta. *Mol. Cell.* 10:417–426. https://doi.org/10.1016/S1097-2765(02)00599-3

Mathys, S., T. Schroeder, J. Ellwart, U.H. Koszinowski, M. Messerle, and U. Just. 2003. Dendritic cells under influence of mouse cytomegalovirus have a physiologic dual role: to initiate and to restrict T cell activation. *J. Infect. Dis.* 187:988–999. https://doi.org/10.1086/368094

Muñoz-Planillo, R., P. Kuffa, G. Martínez-Colón, B.L. Smith, T.M. Rajendiran, and G. Núñez. 2013. $K^+$ efflux is the common trigger of NLRP3 inflammasome activation by bacterial toxins and particulate matter. *Immunity.* 38:1142–1153. https://doi.org/10.1016/j.immuni.2013.05.016

Patsos, G., A. Germann, J. Gebert, and S. Dihlmann. 2010. Restoration of absent in melanoma 2 (AIM2) induces G2/M cell cycle arrest and promotes invasion of colorectal cancer cells. *Int. J. Cancer.* 126:1838–1849. https://doi.org/10.1002/ijc.24905

Poeck, H., M. Bscheider, O. Gross, K. Finger, S. Roth, M. Rebsamen, N. Hannesschläger, M. Schlee, S. Rothenfusser, W. Barchet, et al. 2010. Recognition of RNA virus by RIG-I results in activation of CARD9 and inflammasome signaling for interleukin 1 beta production. *Nat. Immunol.* 11:63–69. https://doi.org/10.1038/ni.1824

Qu, Y., S. Misaghi, K. Newton, A. Maltzman, A. Izrael-Tomasevic, D. Arnott, and V.M. Dixit. 2016. NLRP3 recruitment by NLRC4 during *Salmonella* infection. *J. Exp. Med.* 213:877–885. https://doi.org/10.1084/jem.20132234

Rathinam, V.A., Z. Jiang, S.N. Waggoner, S. Sharma, L.E. Cole, L. Waggoner, S.K. Vanaja, B.G. Monks, S. Ganesan, E. Latz, et al. 2010. The AIM2 inflammasome is essential for host defense against cytosolic bacteria and DNA viruses. *Nat. Immunol.* 11:395–402. https://doi.org/10.1038/ni.1864

Roberts, T.L., A. Idris, J.A. Dunn, G.M. Kelly, C.M. Burnton, S. Hodgson, L.L. Hardy, V. Garceau, M.J. Sweet, I.L. Ross, et al. 2009. HIN-200 proteins regulate caspase activation in response to foreign cytoplasmic DNA. *Science.* 323:1057–1060. https://doi.org/10.1126/science.1169841

Rühl, S., and P. Broz. 2015. Caspase-11 activates a canonical NLRP3 inflammasome by promoting K(+) efflux. *Eur. J. Immunol.* 45:2927–2936. https://doi.org/10.1002/eji.201545772

Sborgi, L., F. Ravotti, V.P. Dandey, M.S. Dick, A. Mazur, S. Reckel, M. Chami, S. Scherer, M. Huber, A. Böckmann, et al. 2015. Structure and assembly of the mouse ASC inflammasome by combined NMR spectroscopy and cryo-electron microscopy. *Proc. Natl. Acad. Sci. USA.* 112:13237–13242. https://doi.org/10.1073/pnas.1507579112

Sun, L., J. Wu, F. Du, X. Chen, and Z.J. Chen. 2013. Cyclic GMP-AMP synthase is a cytosolic DNA sensor that activates the type I interferon pathway. *Science.* 339:786–791. https://doi.org/10.1126/science.1232458

Sutterwala, F.S., Y. Ogura, M. Szczepanik, M. Lara-Tejero, G.S. Lichtenberger, E.P. Grant, J. Bertin, A.J. Coyle, J.E. Galán, P.W. Askenase, and R.A. Flavell. 2006. Critical role for NALP3/CIAS1/Cryopyrin in innate and adaptive immunity through its regulation of caspase-1. *Immunity.* 24:317–327. https://doi.org/10.1016/j.immuni.2006.02.004

Sutterwala, F.S., S. Haasken, and S.L. Cassel. 2014. Mechanism of NLRP3 inflammasome activation. *Ann. N.Y. Acad. Sci.* 1319:82–95. https://doi.org/10.1111/nyas.12458

Tao, J., X. Zhou, and Z. Jiang. 2016. cGAS-cGAMP-STING: The three musketeers of cytosolic DNA sensing and signaling. *IUBMB Life.* 68:858–870. https://doi.org/10.1002/iub.1566

Vance, R.E. 2015. The NAIP/NLRC4 inflammasomes. *Curr. Opin. Immunol.* 32:84–89. https://doi.org/10.1016/j.coi.2015.01.010

Wang, Y., X. Ning, P. Gao, S. Wu, M. Sha, M. Lv, X. Zhou, J. Gao, R. Fang, G. Meng, et al. 2017. Inflammasome activation triggers caspase-1-mediated cleavage of cGAS to regulate responses to DNA virus infection. *Immunity.* 46:393–404. https://doi.org/10.1016/j.immuni.2017.02.011

Wilkins, C., and M. Gale Jr. 2010. Recognition of viruses by cytoplasmic sensors. *Curr. Opin. Immunol.* 22:41–47. https://doi.org/10.1016/j.coi.2009.12.003

Wilson, J.E., A.S. Petrucelli, L. Chen, A.A. Koblansky, A.D. Truax, Y. Oyama, A.B. Rogers, W.J. Brickey, Y. Wang, M. Schneider, et al. 2015. Inflammasome-independent role of AIM2 in suppressing colon tumorigenesis via DNA-PK and Akt. *Nat. Med.* 21:906–913. https://doi.org/10.1038/nm.3908

Wu, J., T. Fernandes-Alnemri, and E.S. Alnemri. 2010. Involvement of the AIM2, NLRC4, and NLRP3 inflammasomes in caspase-1 activation by Listeria monocytogenes. *J. Clin. Immunol.* 30:693–702. https://doi.org/10.1007/s10875-010-9425-2

Wu, J., L. Sun, X. Chen, F. Du, H. Shi, C. Chen, and Z.J. Chen. 2013. Cyclic GMP-AMP is an endogenous second messenger in innate immune signaling by cytosolic DNA. *Science.* 339:826–830. https://doi.org/10.1126/science.1229963

Zanoni, I., Y. Tan, M. Di Gioia, A. Broggi, J. Ruan, J. Shi, C.A. Donado, F. Shao, H. Wu, J.R. Springstead, and J.C. Kagan. 2016. An endogenous caspase-11 ligand elicits interleukin-1 release from living dendritic cells. *Science.* 352:1232–1236. https://doi.org/10.1126/science.aaf3036

Zhao, C., D.D. Gillette, X. Li, Z. Zhang, and H. Wen. 2014. Nuclear factor E2-related factor-2 (Nrf2) is required for NLRP3 and AIM2 inflammasome activation. *J. Biol. Chem.* 289:17020–17029. https://doi.org/10.1074/jbc.M114.563114

Zhong, B., Y. Yang, S. Li, Y.Y. Wang, Y. Li, F. Diao, C. Lei, X. He, L. Zhang, P. Tien, and H.B. Shu. 2008. The adaptor protein MITA links virus-sensing receptors to IRF3 transcription factor activation. *Immunity.* 29:538–550. https://doi.org/10.1016/j.immuni.2008.09.003